Study of Geopolymer Adsorbents Prepared from Metakaolin and Rice Husk Silica for Targeting to Heavy Metal Capture

[重金属捕捉をターゲットとしたメタカオリンと籾殻シリカから成るジオポリマー吸着剤の研究]

LOPEZ GUZMAN FRANCISCO JAVIER

Energy and Environment Science

Nagaoka University of Technology, Nagaoka, Japan

July 2014

Acknowledgment

Foremost, I would like to express my sincere gratitude to my advisor Prof. Dr. Takaomi Kobayashi for the continuous support of my work study and research, for his patience, motivation, enthusiasm, and immense knowledge. His guidance helped me in all the time of research and writing of this thesis. I am thankful for having him as my supervisor has been a great pleasure and honor. Also, I would like to say thank you to my professor Dr. Motohiro Tagaya for his suggestion and support to improve my research work.

I would like to express a very special thank you to my professor Dr. Satoshi Sugita for his support and help to accomplish this goal in my life.

I thank my fellow lab mates for the stimulating discussions, for the sleepless nights we were working together before deadlines, and for all the fun we have had in the last years.

Last but not the least, I would like to thank my friends and more important to my family for giving love and supporting me spiritually throughout my life.

Francisco Javier López Guzmán

Contents

List of Figures

List of Tables

Chapter 1

1.1 Introduction

Emission introduction of hazardous wastes into earth environment has become a worldwide concern due to the accelerated pollution environment by the many anthropogenic interference. Over a period of time, these accumulated pollutants are influenced as potential hazard to human health, animals and ecological environments. To counteract such activities, there are international and national treaties, laws and regulations such as the 1998 International Kyoto protocol, all aimed at strictly finding ways of reducing, monitoring and controlling pollution, and establishing sustainable wastewater treatment strategies.

It was only during the decade of the 1960s, that terms such as *water* and *air pollution*, *protection of environment* and *ecology* became household words. For that reason, many wastewater treatment processes have been developed in analytical instruments such as chromatography, electrodialysis, adsorption, membrane technologies and ion exchange. Some of these processes are very cost effective, whilst others although necessary have high capital and operation costs and the problem of residual disposal. Due to the economic pressures experienced by many companies to reduce operating and maintenance costs, many industries opt for economically feasible processes.

Adsorption and ion exchange processes in water pollution control are with the potential uses of the organic and inorganic polymers. Thus, these materials have been the focus in order to have a solution for this problem.

1.2 Heavy metals as pollutant waste

Heavy metals are elements having atomic weights between 63.5 and 200.6, and a specific gravity greater than 5.0.[1] With the rapid development of industries such as metal plating facilities, mining operations, fertilizer industries, tanneries, batteries, paper industries and pesticides, etc., heavy metals wastewaters are directly or indirectly discharged into the environment increasingly, especially in developing countries. Unlike organic contaminants, heavy metals are not biodegradable and tend to accumulate in living organisms and many heavy metal ions are known to be toxic or carcinogenic. Toxic heavy metals of particular concerned in treatment of industrial wastewaters include zinc, copper, nickel, mercury, cadmium, lead and chromium. Here, lead (Pb) can cause central nervous system damage. Lead can also damage the kidney, liver and reproductive system, basic cellular processes and brain functions. The toxic symptoms are anemia, insomnia, headache, dizziness, irritability, weakness of muscles, hallucination and renal damages.[2]

It is also serious damage in Japan, especially Fukushima, since last earthquake damage. Fukushima nuclear power plants emitted nuclide Cesium^{137} (^{137}Cs), although is not a heavy metal, is a radioactive contaminant concerned in environment with a half-life of 30.4 years . It has been introduced into the environment via various events, notably fallout from the atmospheric weapons testing and accidental release. As an

important source of radioactivity in the radioactive waste, cesium has posed serious environmental threats because of its high solubility and ability to move with aqueous media in the subsurface. Furthermore, as its chemical similarity to potassium, cesium is readily assimilated by terrestrial and aquatic organisms.[3]

Faced with more and more stringent regulations, nowadays heavy metals are the environmental priority pollutants and are becoming one of the most serious environmental problems. So these toxic heavy metals should be removed from the wastewater to protect the people and the environment. Many methods that are being used to remove heavy metal ions include chemical precipitation, ion-exchange, adsorption, membrane filtration, electrochemical treatment technologies, etc.

However, most of these methods are costly and require high levels of expertise, which restricts their application to the end-users. In most cases, the choice of method for wastewater treatment is based jointly on the concentration of heavy metals in solution and the cost of treatment.[4] The adsorption method is one of the most attractive, because its application is relatively simple and safe. As mild operating conditions are used, it is also widely available for abrasion resistant and cheap[5,6]. Also, this methodology presents selective for the heavy metals.

1.3. Adsorption

Adsorption is now recognized as an effective and economic method for heavy metal wastewater treatment. The adsorption process offers flexibility in design and operation and in many cases will produce high-quality treated effluent. In addition,

because adsorption is sometimes reversible, adsorbents can be regenerated by suitable desorption process. Adsorption is a separation process whereby the solute is preferentially removed from a solution by attachment to the surface of the solid, granular material called *adsorbent*. The solute removed is called the *adsorbate*. In adsorbent, attachment of solutes to the solid surfaces happens by bond formation. Depending on the magnitude and origin of the bond formation and the extent of perturbation to the respective electronic structures, the phenomenon of adsorption is broadly classified into two types: physisorption and chemisorption.[7]

The attractive forces in physisorption originate from correlated charge fluctuations that develop when an atom or a molecule is brought into the vicinity of a solid surface. These attractive forces are van der Waals (vdW) forces. The physisorption of molecules or atoms on a solid surface is characterized by largely unperturbed electronic structures of both the adsorbate and the surface. Adsorption of noble gas atoms on metal surfaces is a typical example of physisorption.

On the other hand, the forces that are responsible for chemisorption arise from the overlap of adsorbate and surface. The overlap between adsorbate and adsorbent leads to the formation of new bonds and thus a modification of their electronic structures. The rupture of intramolecular adsorbate bonds and the formation of new surface bonds during chemisorption are crucial steps in any heterogeneous catalysis. The chemisorption of heavy metal on geopolymer surfaces is a focal point of this thesis.

1.3.1. Physisorption

The physisorption of an adsorbate on a solid surface arises from the attractive vdW interactions that are developed when the adsorbate is brought near the solid surface. The cause of this attractive interaction is the quantum mechanical fluctuation of instantaneous dipoles, which originates from the mutual interaction of electrons in the adsorbate and the surface. Here, a neutral atom with a single valence electron is depicted approaching a semi-infinite solid surface with a dielectric constant ε. The interaction of the point charge, *+e* from the nucleus, with the surface induces an image point charge q[8]

$$q = \frac{1-\varepsilon}{1+\varepsilon} e \qquad (1)$$

which is positioned within the solid at the same distance from the surface. Similarly, the interaction of the valence electron (*-e*) induces a corresponding image point charge. This system of point charges and their images constitute the induced dipoles, and are responsible for the attractive forces that arise when the atom is brought near the surface.

1.3.2. Chemisorption

The chemisorption of an adsorbate to a solid occurs when the atoms or molecules are bound to the solid surface through an overlapping of one or more of their electronic orbitals. The formation of chemisorptive bonds between an adsorbate and a solid surface requires electron transfer between them. Depending on the extent of the electron transfer, the chemisorptive bond can be predominantly ionic or

covalent. The first type is characterized by a complete charge transfer between the adsorbate and substrate while the second type is characterized by the sharing of electrons between adsorbate and surfaces.

In the case of molecular chemisorption, particularly diatomic molecules on transition-metal surfaces, it has frequently been observed that the rearrangement of their electronic configuration leads to the dissociation of the molecules to form new adsorbate species. A simple illustration of dissociative chemisorption is the hydrogen on a transition metal surface. The potential energy diagram corresponding to dissociative chemisorption of a neutral diatomic molecule is schematically illustrated in Figure 1.1. The total potential energy curve (a) can be considered as a combination of the physisorption potential from the un-dissociated molecule (b) and the chemisorption potential of two dissociated atoms (c). The dissociative chemisorption of a diatomic molecule can be envisaged to pass through a physisorption well, known as the precursor state before bond dissociation. In Figure 1.1, Q_{diss} is the dissociation energy of the diatomic molecule in the gas phase, E_b is the binding energy of chemisorbed atomic species and *Ed* is the activation energy of desorption. *z* is the distance of the molecule from the surface.

This dissociative chemisorption potential can be described qualitatively as the combination of the potential for a physisorbed molecule and the chemisorption of the corresponding atomic species. A molecule approaching the surface from a large distance, *z*, feels attraction to the surface, which leads to a physisorbed or precursor state. Approaching closer to the surface would cause a rapid increase in the potential

energy of the system due to overlap between molecule's and substrate's electronic states.

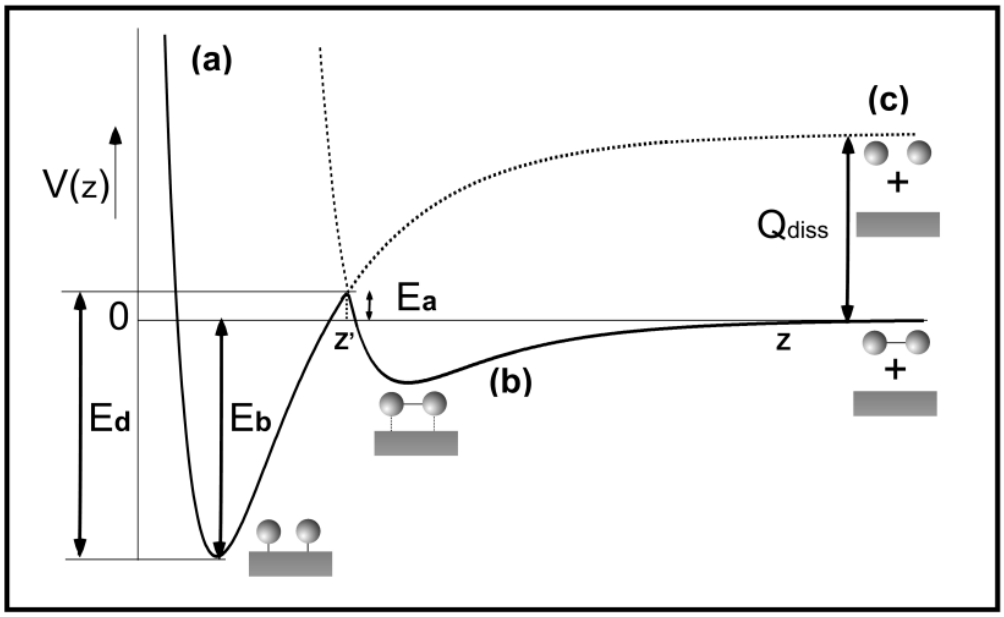

Fig. 1.1. The one-dimensional potential energy diagram corresponding to the dissociative chemisorption of a neutral diatomic molecule on a solid surface.

One experimental distinction between physisorption and chemisorption is that in the chemisorption, one deals entirely with submonolayer adsorption. This is because, in chemisorption the activation energy for adsorption *Ea* for the first monolayer is much greater than that for the succeeding layers. Table 1.1 shows the differences between physisorption and chemisorption.

Table 1.1. Differences between physisorption and chemisorption.

Physisorption	Chemisorption
Occurs only at the temperature below the boiling of the adsorbate.	Can occur at all temperatures.
Heat of adsorption is less than 40 $KJmol^{-1}$	Heat of adsorption can be more than 200 $KJmol^{-1}$
The adsorbed amount increases when the pressure of adsorbate is increasing.	Pressure is insignificant.
The adsorbed amount depends more on the nature of the adsorbate than adsorbent (surface).	The adsorbed amount depends on both the nature of the adsorbent and the adsorbate.
No appreciable activation energy is required.	An appreciable activation energy maybe involved in the process.
Multilayer adsorption occurs.	Only the monolayer adsorption occurs.

Ion exchange is a chemisorption process, whereas adsorption may be physisorption or chemisorption. The ion exchange reaction may be defined as the reversible interchange of ions between a solid phase (the ion exchanger) and a solution phase. The ion exchanger is usually insoluble in the medium in which the exchange is carried out. All of ion exchange processes are extremely rapid and they follow the general well known kinetic laws as shown in the equation below. The following reaction illustrates the interactions between the solid phase and the ions in solution;

Cationic Exchanger

$$M^{-}A^{+}_{(solid)} + B^{+}_{(solution)} \leftrightarrow M^{-}B^{+}_{(solid)} + A^{+}_{(solution)} \quad (2)$$

Ion exchange is an important process due to it is able to achieve complete demineralization[9], through simultaneous cation and anion exchange.

The uptake of heavy metals in wastewater treatment is attributed to both mechanisms of ion exchange and the adsorption process. However, the sorption processes of ion exchange and adsorption are unit operations, which often share theory[10]. However, adsorption is the accumulation of materials at an interface, and this interface may be liquid–liquid, liquid–solid, gas–liquid or gas–solid. Ion exchange process becomes similar to an adsorption system in which a solid, usually porous particle with reactive sites on its surface comes into equilibrium with ions in solution. These reactive sites have exchangeable ions such as Na^{+}, H^{+}, Cl^{-}, OH^{-} attached, and these ions exchange with ions in solution at equilibrium. Adsorption is mainly applicable in wastewater treatment whereas ion exchange is used in water treatment. Nowadays, exist different types of adsorbents material used for wastewater treatment, some of them are activated carbon, fuller earths, activated clays, bauxite, silica gel, resins, zeolites, etc.

It is known that activated carbon (AC) adsorbents are widely used in the removal of heavy metal contaminants. Its usefulness derives mainly from its large micropore and mesopore volumes and the resulting high surface area. A large number

of researchers are studying the use of AC for removing heavy metals.[11] Nowadays, the depleted source of commercial coal-based AC results in the increase of price. To make progress in heavy metals adsorption to AC without the expense of decline in the pollutants adsorption, additives and AC composite could be an option. Additives of alginate,[12] tannic acid,[13] magnesium,[14] surfactants,[15] and AC composite could be effective adsorbents for heavy metals (Table 1.2). And searching for alternative AC from abundant and inexpensive sources is of concern. Converting carbonaceous materials into AC for heavy metals remediation have been reported. Dias et al.[16] reviewed the waste materials for AC preparation. Kongsuwan et al.[17] explored the use of AC from eucalyptus bark in the binary component sorption of Cu^{2+} and Pb^{2+}. The maximum sorption capacities for Cu^{2+} and Pb^{2+} were 0.45 and 0.53 mmol/g. A major mechanism for the uptake of both heavy metals was proven to be adsorption.

AC has been the most used adsorbent, nevertheless it is relatively expensive. Searching for low-cost and easily available adsorbents to remove heavy metal ions have become a main research focus. To date, hundreds of studies on the use of low-cost adsorbents have been published. Agricultural wastes, industrial byproducts and wastes and natural substances have been studied as adsorbents for the heavy metal wastewater treatment. Several reviews are available that discuss the use of low-cost adsorbents for the treatment of heavy metals wastewater. Bhattacharyya and Gupta[18] reviewed the adsorption of a few heavy metals on natural and modified kaolinite and montmorillonite. Sud et al.[19] reviewed agricultural waste material as potential adsorbent for sequestering heavy metal ions from aqueous solutions. Wan Ngah and Hanafiah[20] reviewed the removal of heavy metal ions fromwastewater by chemically

modified plantwastes as adsorbents. Babel and Kurniawan[21] reviewed the use of lowcost adsorbents for heavy metals uptake from contaminated water. Researchers investigated industrial by-products such as lignin, diatomite,[22] lignite, aragonite shells,[23] natural zeolites,[24], clay,[25] kaolinite,[26] and peat,[27] etc. Jiang et al.[28] investigated the kaolinite clay obtained from Longyan, China to remove heavy metal ions Pb(II), Cd(II), Ni(II) and Cu(II) from wastewater. The uptake is rapid with maximum adsorption being observed within 30 min. And kaolinite clay was used for removing metal ions from real wastewater containing Pb (II), where its concentration was reduced from 160.00 mg/L to 8.00 mg/L. Agoubordea and Navia[29] reported zinc and copper removal from aqueous solutions using brine sediments, sawdust and the mixture of both materials. The maximum adsorption capacity was found to be 4.85, 2.58 and 5.59 mg/g for zinc and 4.69, 2.31 and 4.33 mg/g for copper, respectively, using an adsorbent/solution ratio of 1/40.

Biosorption of heavy metals from aqueous solutions is a relatively new process that has been confirmed a very promising process in the removal of heavy metal contaminants. The major advantages of biosorption are its high effectiveness in reducing the heavy metal ions and the use of inexpensive biosorbents. Biosorption processes are particularly suitable to treat dilute heavy metal wastewater. Typical biosorbents can be derived from three sources as follows:[17] (1) non-living biomass such as bark, lignin, shrimp, krill, squid, crab shell, etc.; (2) algal biomass; (3)microbial biomass, e.g. bacteria, fungi and yeast. Different forms of inexpensive, non-living plant material such as potato peels,[30] sawdust,[31] black gram husk,[32] seed shells,[33] coffee husks,[34] sugar-beet pectin gels,[35] and citrus peels,[36] etc., have been widely

investigated as potential biosorbents for heavy metals. Algae, a renewable natural biomass proliferates ubiquitously and abundantly in the littoral zones of world has attracted the attention of many investigators as organisms to be tested and used as new adsorbents to adsorb metal ions. Several advantages in applying algae as biosorbent include the wide availability, low cost, high metal sorption capacity and reasonably regular quality.[37] Moreover, the separation of biosorbents would be difficult after adsorption.

Table 1.2. Heavy metal ion adsorbents

Adsorbent	**Heavy metal**	**Reference**
Activated carbon	Cd^{2+} and Pb^{2+}	11
AC-alginate	Pb^{2+}, Mn^{2+}, Cd^{2+}, Cu^{2+}, Zn^{2+}, Fe^{2+}, Al^{3+} and Hg^{2+}	12
Tannic acid	Cu^{2+}, Cd^{2+}, Zn^{2+}, Mn^{2+} and Fe^{3+}	13
Magnesium	Zn^{2+} and Cd^{2+}	14
Surfactants	Cd^{2+}	15
Shells	Cd^{2+}	23
Natural zeolites	Cu^{2+}, Cd^{2+}, and Pb^{2+}	24
Peat	Cu^{2+}, Ni^{2+} and Cd^{2+}	27
Kaolinite	Cd^{2+}, Cu^{2+}, Ni^{2+}, Pb^{2+} and Zn^{2+}	26
Potato peels	Cu^{2+}	30
Sawdust	Pb^{2+}	31
Black gram husk	Cd^{2+}, Cu^{2+}, Ni^{2+}, Zn^{2+} and Pb^{2+}	32
Coffee husks	Dye contaminated waters.	34
Sugar-beet pectin gels	Cd^{2+}, Pb^{2+} and Cu^{2+}	35

1.4. Geopolymer adsorbents

Geopolymers, also can be used as material for removing heavy metals from wastewater via adsorption. They could become a new method for industries, consequently affecting both the environment and societies positively. In recent years, the adsorption of methylene blue dye on a fly ash based geopolymer adsorbent was study, as demonstrated with an adsorption capacity of approximately 0.12 mmol/g[38]. Fly ash-based geopolymer was used for Cu^{2+} removal from an aqueous solution. The adsorption capacity reached 92 mg/g, which is a significantly higher value than those of fly ash and natural zeolite[39]. The effects of zeolitic were implemented as filler on the mechanical performance. The adsorption capacity of geopolymer products was confirmed that natural zeolitic could become stable geopolymers with high mechanical properties and high adsorption capacity regarding methylene blue and Cu^{2+}[40]. However, existing literature on the adsorption of heavy metals using geopolymers is scant.

Geopolymers present high adsorption capacity of heavy metal in water.[60–62] However, existing literature on the adsorption of heavy metals using geopolymers has not seen in research study. The selectivity order of geopolymers for metal ions is usually brought about by the various factors that influence adsorption and ion exchange behaviour in geopolymers. This brings about effects such as the sieving effect for metal ions or the availability of the specific exchange sites in the geopolymer. Depending on the arrangement of the geopolymer amorphous lattice or pore volumes, the incoming ions will be affected, and may diffuse through the structure or fail to

move through the pores. Most researchers have found different cation exchange capacities and interestingly, it was noted that geopolymers exhibits different selectivity series for different metal ions. A summary of geopolymer adsorbents are in table 1.3.

Table 1.3. Geopolymer as adsorbents.

Geopolymer type	Selectivity series	Reference
Metakaolin-based geopolymer	$Pb^{2+} > Cd^{2+} > Cu^{2+} > Cr^{3+}$	42
Zeolite-based geopolymer	Ni^{2+}, Cu^{2+}, $Zn^{2+} > Cd^{2+}$, Pb^{2+}	43
Fly ash-based geopolymer	Methylene blue, crystal violet and Cu^{2+}	38,39

Metakaolin-based geopolymer could adsorb different heavy metals (i.e., Pb^{2+}, Cu^{2+}, Cr^{3+}, Ni^{2+}, Zn^{2+} and Cd^{2+}). However, of the metals tested, optimal adsorption with the implementation of the geopolymer occurred with Pb^{2+}.[42,44] This discovery may facilitate the development of optimized procedures for wastewater treatment, thus providing an alternative solution to environmental damages caused by heavy metal pollutants.

pH is a very important controlling parameter in adsorption and ion exchange processes. Chemically, a change in solution pH influences metal speciation leading to the formation of complex inorganic species in solution. The exact speciation (the metal ion complex that predominates at a particular solution pH) of a metal has a significant impact on the removal efficiency and its selectivity. The presence of

precipitates in solution, usually clog the geopolymers and hinder metal ion accessibility of sites.

1.4.1. Geopolymer matrices

In 1979, Dr. Davidovits created and applied the term *geopolymer* to represent an inorganic polymer constituted by SiO_4 and AlO_4 tetrahedra being the structural units[45]. These inorganic polymers are formed by the reaction of polycondensation between an alkaline solution as sodium hydroxide and sodium silicate with an aluminosilicate source as metakaolin (MK), fly ash, rice husk ash (RHA) and slag, just to mention some. Nowadays, geopolymers are receiving a lot of attention because they may be used as a viable economical alternative to inorganic cements in diverse applications, such as military, aircraft[46,47], high-tech ceramics, thermal insulating foams, fire-proof building materials[48], protective coatings[49], refractory adhesives and hybrid inorganic-organic composites[50,51]. This interest is due to their exceptionally high thermal and chemical stability, excellent mechanical strength, adhesive behavior and long-term durability. In addition, early researchers have demonstrated that geopolymers are cheap to produce and can be made from a great number of minerals and industrial by-products, including pozzolana[52,53], natural aluminosilicate minerals[54], MK[41,55,56], fly ash[57], granulated blast furnace slag[58], fly ash and kaolinite mixture[59], fly ash and MK mixture[60,61], red mud and MK mixture and red mud and fly ash mixture.

Geopolymer has a similar composition of zeolitic materials. However, the microstructure of geopolymeric material is a three dimensional silico-aluminate

amorphous or semiamorphous structure instead of crystalline[54,62,63], consisting of linked SiO_4 and AlO_4 tetrahedra by sharing all the oxygen atoms and described by the following empirical formula:

$$M_n^+[-(SiO_2)_z - AlO_2 -]_n \quad (3)$$

where M^+ is an alkali cation (Na^+, K^+ or Ca^{2+}) necessary for balancing the negative charge of Al^{3+} in IV-fold coordination; z is the Si/Al ratio and n is the degree of polymerization, which can be designated as four types depending of the atomic ratio of Si/Al,

Si/Al = 1	poly-sialate (PS)	(-Si-O-Al-O-)
Si/Al = 2	poly-sialate-siloxo (PSS)	(-Si-O-Al-O-Si-O-)
Si/Al = 3	poly-sialate-disiloxo (PSDS)	(-Si-O-Al-O-Si-O-Si-O-)
Si/Al = 4	poly-sialate-multisiloxo (PSMS)	Consist of siloxonate, silanol and sialate chains

where *sialate* is an abbreviation for silicon-oxo-aluminate. Geopolymers exhibit different properties according to the Si/Al ratio. Geopolymers with Si/Al ≤ 3 result in three-dimensional cross-linked rigid networks with stiff and brittle properties as cements or ceramics materials; and geopolymers with Si/Al > 3 results in 2-D networks and linearly linked polymeric structures with adhesive and elastic properties.

1.4.2. Characteristics in geopolymers.

Geopolymer chemistry is associated with that of zeolites, since they have comparable chemical composition[64]. The difference in these materials is that geopolymers present an amorphous structure in comparison with the highly crystalline structure of zeolites. Nowadays, geopolymers are understood as alkaline activated aluminosilicates or an inorganic 2-component system, consisting of a reactive solid component that contains SiO_2 and Al_2O_3 in sufficient amounts and in reactive form as ashes, active clays, pozzolana, slags, etc. In these systems, alkaline activation solution contains individual alkali hydroxides, silicates, aluminates, carbonates, and sulphates or combinations thereof.

The reaction between these species is the polycondensation process leading to the formation of amorphous to semi-crystalline aluminosilicate polymers. The schematic formation of geopolymer material can be shown as illustrated by the following two reactions[54]:

$$\underset{\text{Aluminosilicate (raw material)}}{n(SiO_2,Al_2O_2)} + 2nSiO_2 + 4nH_2O + MOH \rightarrow M^+ + \underset{\text{Geopolymer precursor}}{n(OH)_3{-}Si-O-\overset{\overset{Al^-}{|}}{\underset{\underset{(HO)_2}{|}}{}}-O-Si-(OH)_3} \quad (4)$$

$$n(OH)_3{-}Si-O-\overset{\overset{Al^-}{|}}{\underset{\underset{(HO)_2}{|}}{}}-O-Si-(OH)_3 + MOH \rightarrow (M^+)-\underset{\text{Geopolymer}}{(-\overset{\overset{|}{O}}{\underset{|}{Si}}-O-\overset{\overset{|}{O}}{\underset{|}{Al^-}}-O-\overset{\overset{|}{O}}{\underset{|}{Si}}-O-)} + 4nH_2O \quad (5)$$

M = Na^+, K^+ or combination of them

The above two reactions suggest that any materials contain mostly silica and alumina in amorphous form which is a possible source for the production of geopolymers with excellent mechanical properties as well as largely amorphous structure. This has average density of 2 g/ml, average of compressive strength of 35 MPa and high resistance of acids. However, defining a representative formulation for geopolymers is quite an impossible labor.

In geopolymer preparation, stoichiometric amounts of MK, fly ash or other starting materials are added to activation solution. The activation solution is pre-made by mixing the required amounts of water, alkaline solution and leaving it to cool naturally to room temperature. Here, the mixture is mixed for 15 minutes, followed by 15 minutes of vibration, which allows for the escapement of excess air. Then, the mixture is poured into completely seald PVC mould and cured at 40° C for approximately 20 hours, depending on the type of experiment, and stored until equilibrium is reached.

1.4.3. Geopolymerization

Geopolymerisation is an exothermic process that is carried out through oligomers (dimer, trimer) which provide the actual unit structures for the three dimensional macromolecular edifice. Figure 1.2 shows the conventional preparation of geopolymer.

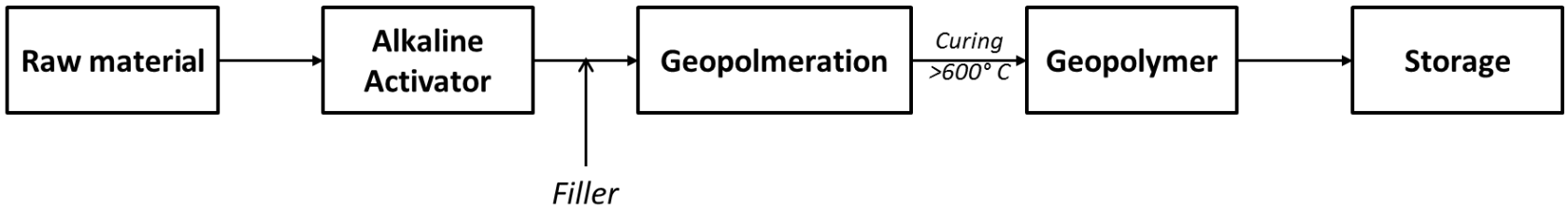

Fig. 1.2. Procedure used for the preparation of geopolymer materials

One of several hardening mechanisms involves the chemical reaction of alumino-silicate oxides with alkalis and alkali–polysilicates yielding polymeric Si–O–Al bonds with a $(Si_2O_5,Al_2O_2)_n$ formula. This is accomplished by calcining alumino-silicate hydroxides $(Si_2O_5,Al_2(OH)_4)$ through the reaction:

$$2(Si_2O_5,Al_2(OH)_4) \rightarrow 2(Si_2O_5,Al_2O_2)_n + 4H_2O \quad (6)$$

or by condensation of SiO and Al_2O vapours according to reaction:

$$4SiO_{(vapour)} + 2Al_2O_{(vapour)} + 4O_2 \rightarrow (Si_2O_5,Al_2O_2)_n \quad (7)$$

which produces also condensed silica fume and corundum:

$$2SiO + O_2 \rightarrow 2SiO_2 \text{ and } Al_2O + O_2 \rightarrow Al_2O_3 \quad (8)$$

The basic steps of geopolymerisation involve dissolution of solid alumino-silicate oxides in MOH solution (M: alkali metal), diffusion or transportation of dissolved Al and Si complexes from the particle surface to the inter-particle space, formation of a gel phase resulting from the polymerization between added silicate solution and Al and Si complexes and finally hardening of the gel phase. The formation of $[M_z(AlO_2)_x(SiO_2)_y{\cdot}nMOH{\cdot}mH_2O]$ gel essentially relies on the extent of dissolution of alumino-silicate materials, while geopolymers with amorphous structure are formed

during reaction[65]. The time required for the alumino-silicate solution to form a continuous gel depends on raw material processing conditions.

Dissolution of the starting materials is the major step that has a twofold role. Firstly, polysialate forming species are liberated from the starting materials in a similar way in the formation of zeolite precursors[56]. Secondly, in the dissolution activates the surface and binding reactions take place contributing significantly to the final strength of the structure. The extent of the dissolution step in geopolymerisation is not fully clear while the extent to which other factors complement or not dissolution needs to be further examined.

Under alkaline conditions, alumino-silicates are transformed into extremely reactive materials. It is generally believed that the dissolution process is initiated by the presence of hydroxyl ions. Higher amounts of hydroxyl ions facilitate the dissociation of different silicate and aluminate species, promoting thus further polymerisation[66]. However, if a very high alkaline environment (>30 mol% overall Na_2O content) is used, the connectivity of silicate anions may be reduced resulting thus in poor polymerization[67].

1.4.4. Structure of Geopolymer

The conceptual models of geopolymerisation published in the literature. There are two broad categories in zeolite analogue and glass models. It is critical to have an accurate conceptual and structural model for the material formation process and properties at lower temperatures. However, each of these views stems from different

underlying principles, and predicts differing response of geopolymers to exposure to high temperatures. The structure of geopolymers is often described broadly by the term X-ray amorphous. The major feature of powder X-ray diffraction (XRD) patterns of geopolymers is a featureless *hump* centred at approximately 27-29° of 2θ.[80] However, it is possible to obtained a formation of semicrystalline or polycrystalline phase on several occasions,[54,55,59,63,68] particularly where no soluble silicon is present in the alkali activating solution.

The level of detailed geopolymer characterisation is generally poor in the literature. Indeed, the elaboration of structural models for geopolymers is not easy and theoretical work is necessary for understanding the chemical reactions involved in the geopolimerization. Figure 1.3 displays the structural models for different geopolymers proposed by Davidovits[55].

The geopolymers as precursors of zeolites has a similar framework of SiO_4 and AlO_4. However, the geopolymers are amorphous materials while the zeolites presented a crystallinity in their framework[62]. Figure 1.4 gives a schematic view on the geopolymer framework and the framework of zeolite.

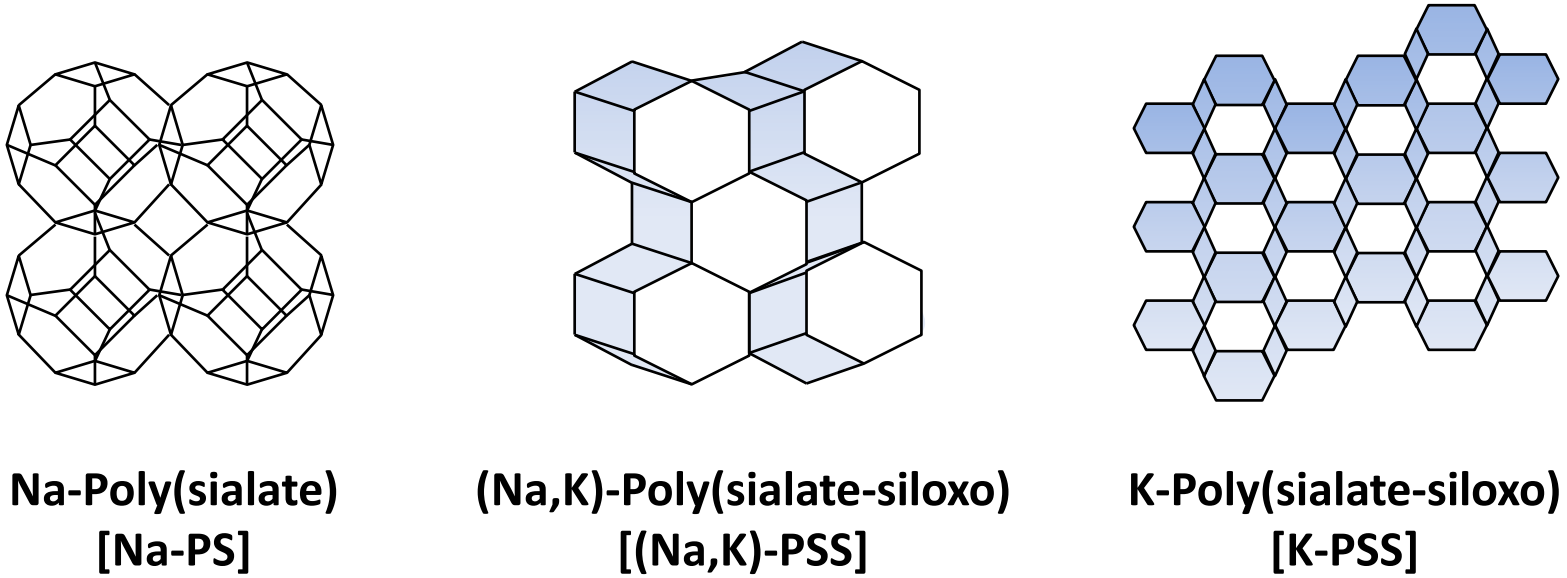

Fig. 1.3. Structural models of geopolymers from Davidovits (1991)

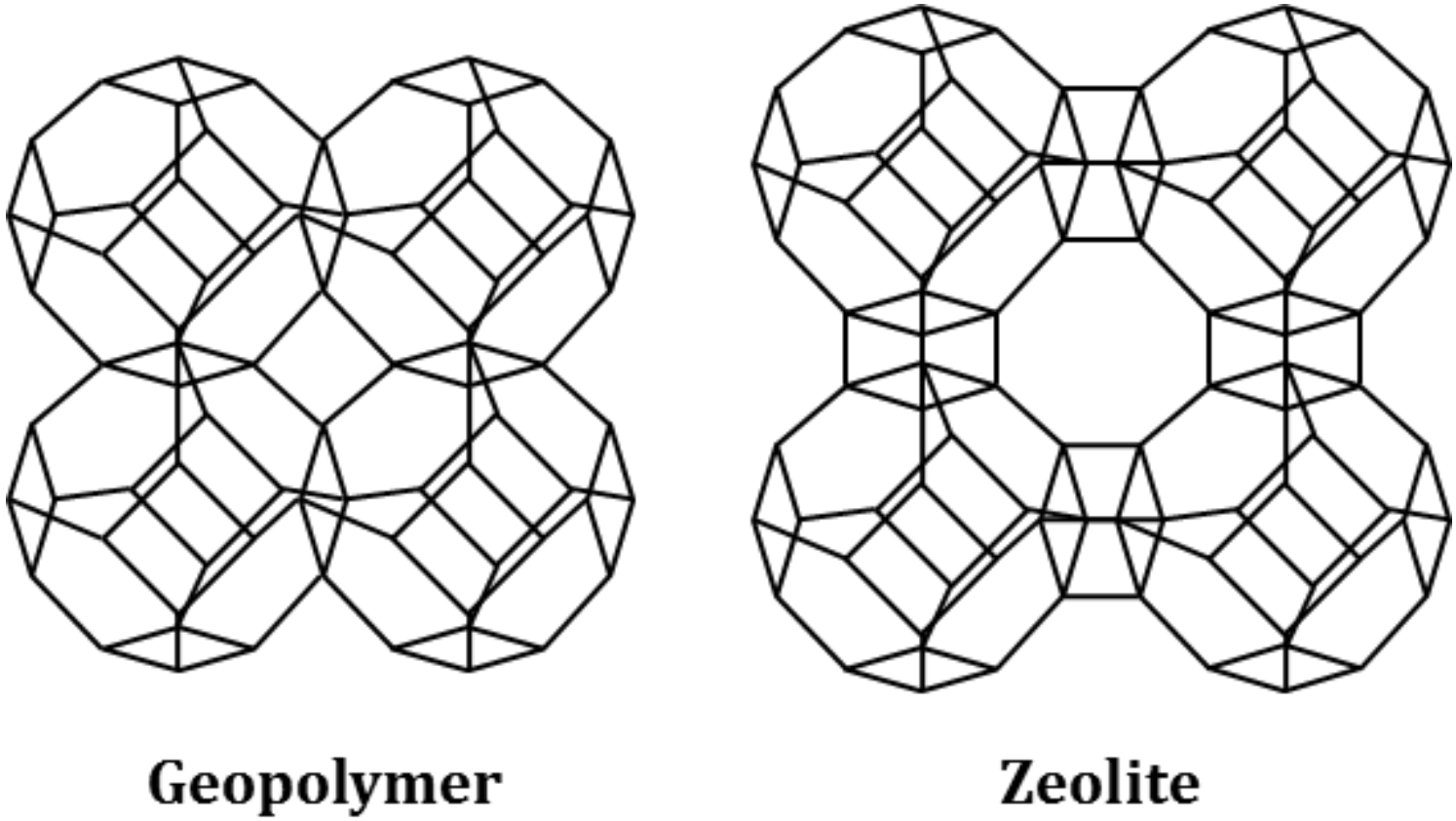

Fig. 1.4. Structure scheme of frameworks of geopolymer and zeolite.

Geopolymers are comprised of cations of Si^{4+} and Al^{3+} linked together by oxygen anions, O^{2-}. Here, the geopolymerization process forms aluminosilicate frameworks, which composes of a large amount of monomers as the main compositions and free water when the polycondensation is carried out at temperatures below 150-200° C as shown in semi-schematic structure for geopolymer Na-PS in Figure 1.5.[64] As mentioned in the early stages of the reaction, the conceptual model for geopolymerization proposed by Duxson et. al.[56] are presented in Figure 1.6. The speed of formation of dissolved monomers is greater than the speed of precipitation of the gel. It involves free Al-OH groups that will later with time or with temperature evidently polycondense with opposed Si-O-Na, into sialate bonds.

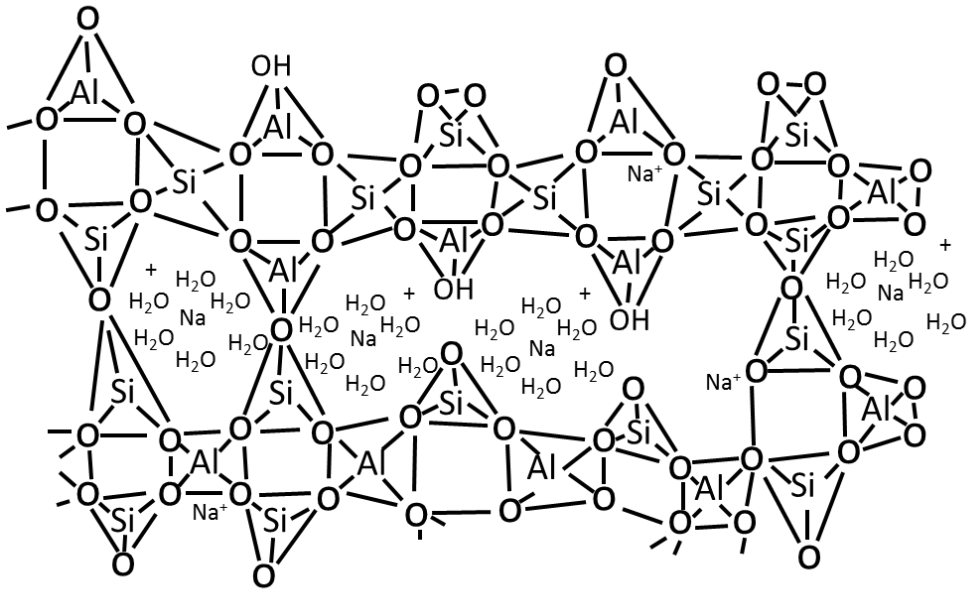

Fig. 1.5. Proposed semi-schematic structure for Na-polysialate geopolymer.

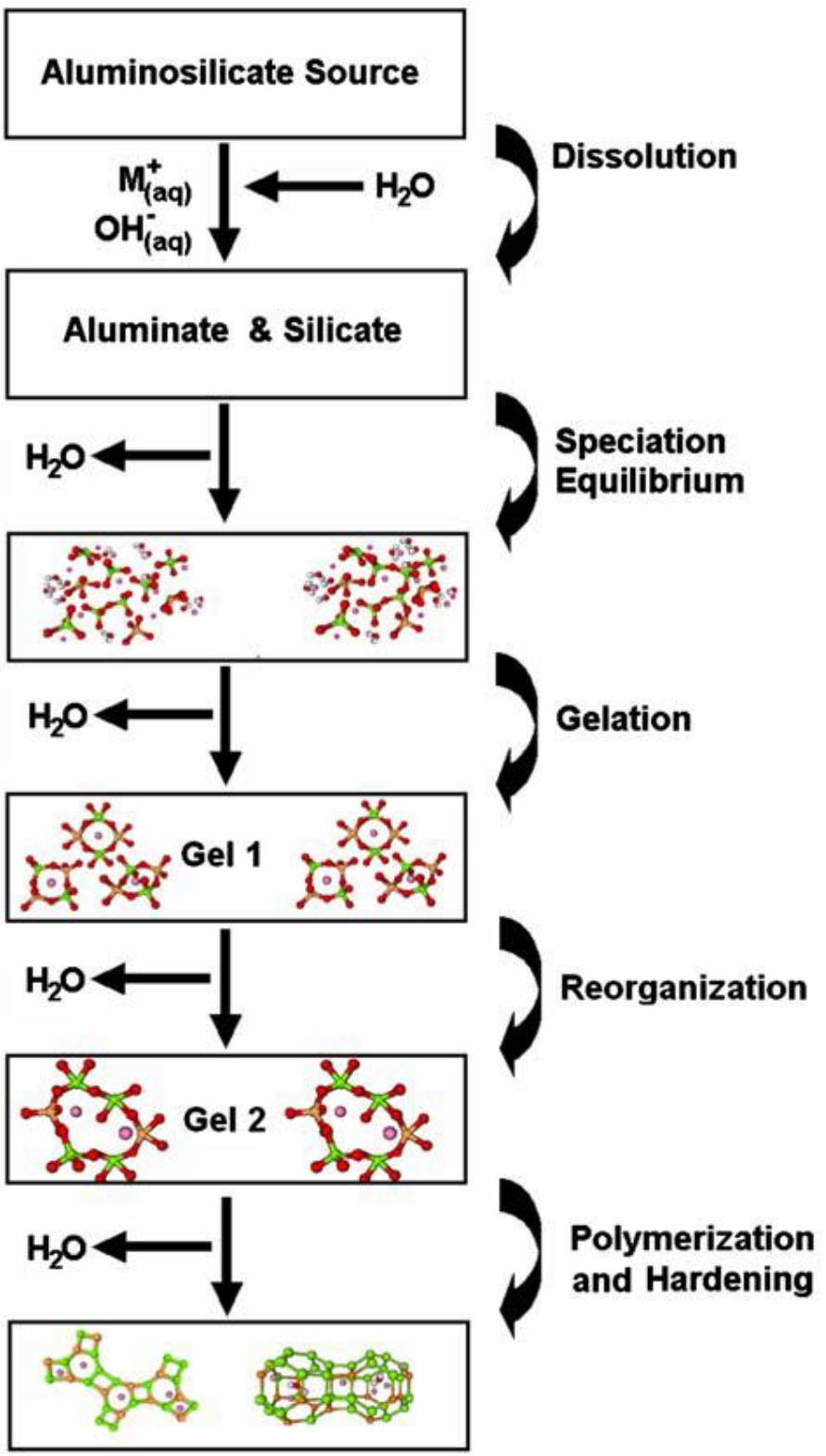

Fig. 1.6. Conceptual model for geopolymerization.[56]

1.4.5. Chemical characterization of Geopolymers

Analytical advanced techniques may be used to obtain maximum information and elucidate geopolymerisation mechanisms. The ability of Al–Si minerals to undergo geopolymerisation may be predicted by specific surface area measurements, which provide an indication of how much surface area participates in heterogeneous reactions within a solid–fluid system. Optical microscopy provides a visual description of the microstructure, since it shows in scale the physical size and shape of the various components of geopolymers. X-ray fluorescence (XRF) spectrometry may be used for elemental analysis of Al–Si minerals. X-ray diffraction (XRD) may be also a useful tool even though the amount of information which can be obtained is limited due to the substantial amorphous nature of geopolymers. However it does provide information regarding the extent to which crystalline starting materials have reacted.[69] Previous experimental studies mentioned the presence of hydrosodalite formed when kaolinite or other phyllosilicates as montmorillonite or halloysite react with a concentrated NaOH solution at 100° C[70]. In the most of the case, geopolymers contain small amounts of crystalline elements from the raw material such as muscovite, titanium oxide, quartz, corundum, haematite, kaolinite, etc. However, geopolymers remain an X-ray amorphous.

Infrared spectroscopy (IR) is a useful as analytical technique used for both qualitative and quantitative methods for of mainly organic and inorganic materials. IR applies radiation of ~1 μm wavelength to provide information about the vibrational transitions and rigidity of chemical bonds found in the all alluminosillicates, which are

assignaed to internal vobrations of Si-O-Si, Si-O-Al and are found at 1250-950 cm^{-1} and 500-420 cm^{-1}. The stretching mode are sensitive to the Si:Al composition of the framework and may shift to lower frequency with increasing number of thetrahedral aluminum atoms. Table 1.4 shows some of the characteristic bands and corresponding vibrations of IR spectra for geopolymers.

Table1. 4. Corresponding vibrations of IR spectra for geopolymers.

Vibration	[cm^{-1}]	Mode
Si-O	1100-1080	Symmetry vibration
Si-O-Al	1008	Asymmetry vibration
Al–O-H	914	Stretching vibration, VI coordinated
Si–O-H	840	Bending vibration
Al-O	798	Stretching vibration, IV coordinated
Si-O	694	Symmetrically stretching vibration
Si-O-Al	540	Bending vibration
Si-O	469	In-plane bending vibration

This method of investigation is complementary to X-ray structural analysis.

1.4.6. Properties and application of geopolymers.

Microsturcture and properties of geopolymers depend strongly on the nature of the initial raw materials.[56] Through microstructural investigations it becomes clear that the ratio of the starting materials influences the homogeneity of the geopolymer

microstructure, which in turn affects thermal conductivity and compressive strength.[71]

The synthetic geopolymers as thermo-setting organic resins are stable up to 1000–1200° C. These products possess properties such as hard surfaces (4 to 7 on the Mohs scale), thermal stability, high surface smoothness and precise mouldability, thus can be useful for tooling, moulding art objects, ceramics as well as building materials. Geopolymers harden rapidly at room temperature and may acquire compressive strength in the range of 20 MPa after only 4 h, after 28 days the compressive strength may reach 70 to 100 MPa.[72]

The unique properties of the geopolymeric materials apart from high early strength, include also low alkali-aggregate expansion, freeze–thaw, sulphate and corrosion resistance. Geopolymers tested for encapsulation of toxic wastes proved quite efficient due to their minimal response to acid leaching.

Geopolymeric cements and concretes show low shrinkage in air after drying, preventing thus formation of cracks. The properties of inorganic polymer concretes are similar to Portland cement-based concretes and depend upon the mix design and curing technique[73]. It is of high importance to study under certain working conditions the compatibility between the C–S–H gel (formed during hydration of the OPC) and the geopolymer gel[56,74]. These advantages make geopolymerisation a promising technology for new construction materials even though the cost for manufacturing Portland cement is relatively low. Therefore, the production of fly ash-based geopolymer concrete could be 10–30 % cheaper than that of Portland cement

concrete. Moreover, since geopolymers can be made from recycled mineral wastes, the introduction and wide use of low CO_2 geopolymeric cements would reduce carbon-dioxide emissions from the cement and concrete industries by almost 80 %.

The applications of geopolymeric binders have been tested in pilot studies worldwide. Some products have reached industrial applications, such as new class of special and blended cements, building products, advanced mineral binders for severe environments, temperature stable resins for moulds and forms and ceramic–ceramic composites.

Immobilisation techniques are used for the treatment of large amounts of heavy metals and radioactive wastes, thus geopolymerisation has received over the years significant attention due to its low cost, flexibility and increased durability versus time[55]. Geopolymers have already been used to immobilize and stabilise low-level radioactive wastes in pure or mixed forms as well as heavy metals[75]. It is known that geopolymers behave similarly to zeolites which are known for their ability to the encapsulation of toxic ions. Geopolymers act as a binder to convert semi-solid waste into an adhesive solid and also immobilise hazardous wastes containing elements such as arsenic, mercury and lead by locking them within the three dimensional framework. Their Ionic size and valence of specific ions are believed to be two of the main factors that influence the incorporation of this ion into the geopolymeric matrix; ionic size correlates well with immobilisation efficiency.

Apparently it is suggested that the chemical bonding plays insignificant role in the immobilization mechanism. Therefore the metals are believed to be

microencapsulated as hydroxide or monomeric/small chain silicate species within the Al- and Si-rich amorphous phase of geopolymers[76]. The heavy metals present in the waste mass seem to affect the chemical and physical characteristics of the final product, while the concentration of the alkali activator influences the immobilisation behavior of a geopolymeric system[77].

In general, the atomic ratio Si/Al in the poly(sialate) structure determines the properties and application fields. A low ratio Si/Al < 3 initiates a 3D-Network that is very rigid. A high ratio Si/Al > 15, provides polymeric character to the geopolymeric material. Figure 1.7 shows different applications of geopolymers depending the ratio of Si/Al.

1.5. Raw Materials Used to Make Geopolymers.

As mentioned, geopolymers can pepared from several natural sources (Table 1.5). Among them, in the present work, raw material used toi prepare geopolymers are chosen from metakaolin and rice husk ash as followed,

1.5.1. Metakaolin (MK)

Kaolinite is a clay mineral with the chemical composition $Al_2Si_2O_5(OH)_4$, formed by tetrahedral silica layer (SiO_4) and one octahedral alumina layer $AlO_2(OH)_4$ as shows in Figure 1.8. The ideal chemical composition of kaolinite is SiO_2 46.51%, Al_2O_3 39.53% and H_2O 13.96%.[78–80] Kaolinite mineral has the cation exchange capacity (CEC); the values for this mineral has a typically range between 3 to 15 meq/100 g.

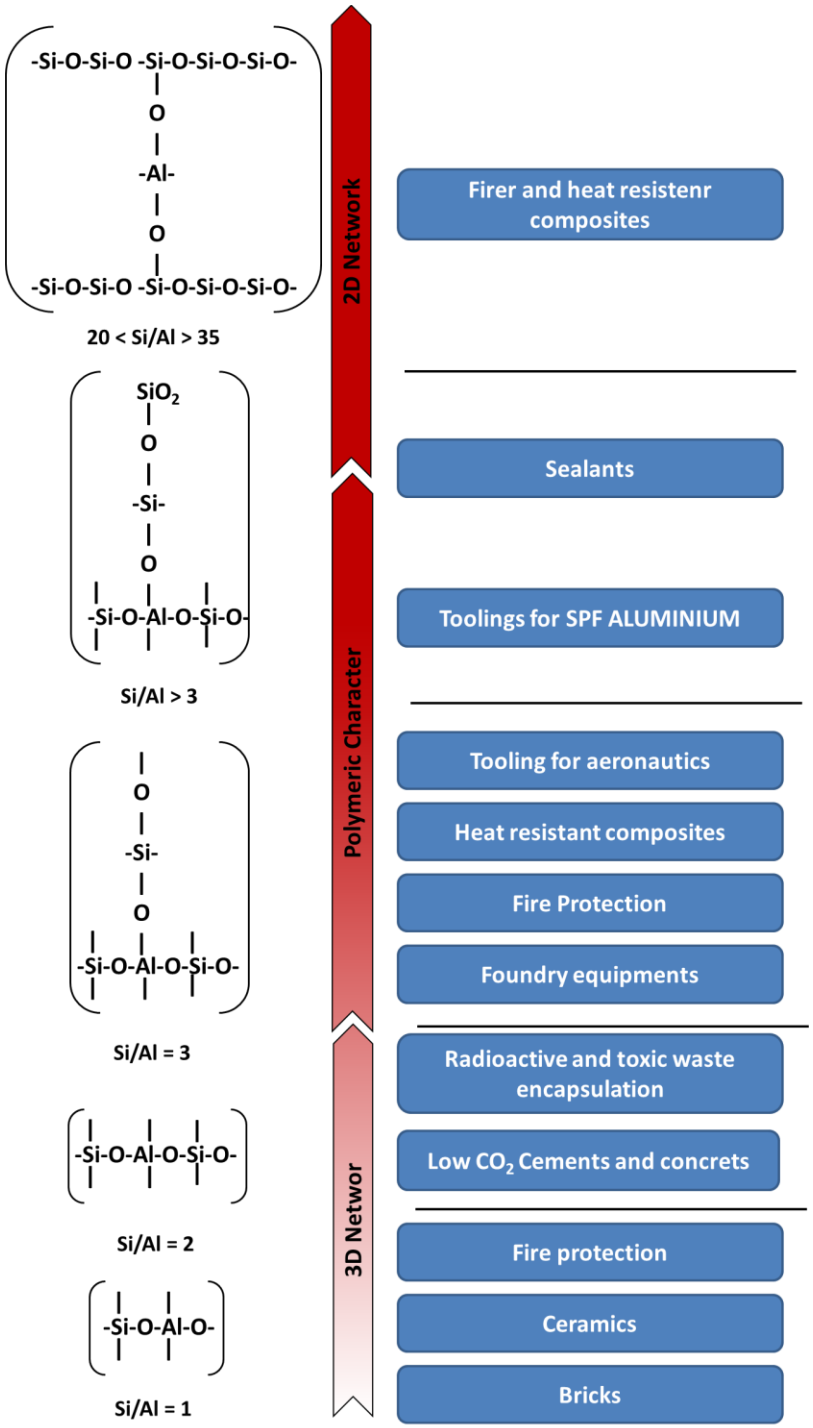

Fig. 1.7. Geopolymer types involved in successful application.

Table 1.5. Natural source raw material for geopolymer

Raw material	Reference
Fly ash	[38,57,59,60,66]
Metakaolin	[42]
Zeolite	[43]
Rice Husk Ash	[44]
Pumice-type	[52]
Kaolinie	[59]
Slag	[69]
Stilbite	[81]

Kaolinite also has a low shrink-swell capacity. It is a soft, earthy, usually white mineral, produced by the chemical weathering of aluminum silicate minerals like feldspar. Rocks that are rich in kaolinite are known as china clay, white clay, or kaolin. Kaolin is a fine, white, clay mineral that has been traditionally used in the manufacture of porcelain. It is thought that the term kaolin is derived from the Chinese Kaoling.

MK is a highly pozzolanic and reactive material produced by the dehydroxylation of the kaolinite minerals, following the next reaction [82]:

$$Al_2Si_2O_5(OH)_4 \xrightarrow{\Delta} Al_2O_3 \cdot SiO_2 + H_2O \quad (9)$$

The dehydroxilization of kaolinite to MK is an endothermic process due to the large amount of energy required to remove the chemically bonded hydroxyl ions, which breaks down the crystal structure producing a transition phase, which correspond to silica and amorphous alumina in reactive form, with high surface area; this process occurs in the range of 500-800°C[83]; burning at higher temperature will cause recrystallization into quartz and mullite transition. MK has twice of the reactivity of most other pozzolans materials and is a valuable admixture for concrete/cement and ceramic applications. Many researchers have focused on the manufacture of geopolymeric products and their industrial applications by using MK as the main reactant.[48,68,81,84]

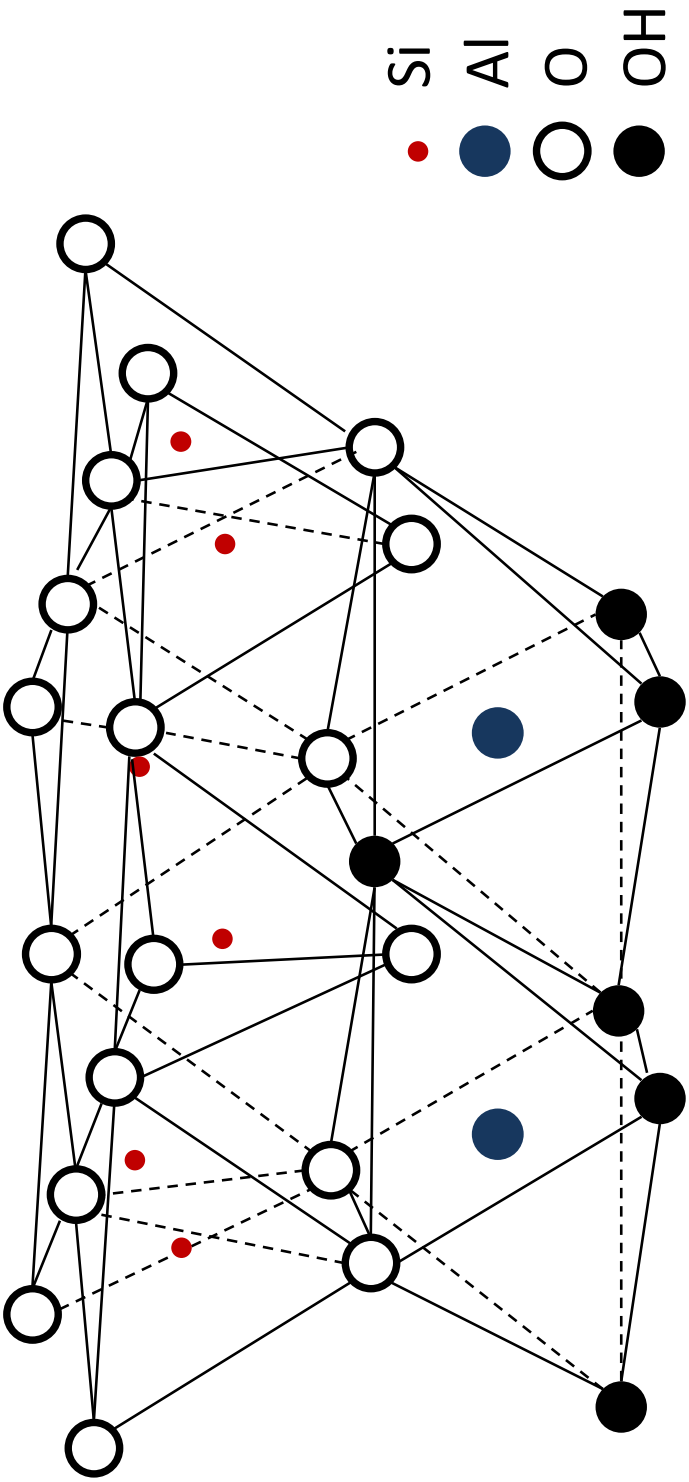

Fig. 1.8. Structure of a kaolinite layer.

1.5.2. Rice Husk Ash (RHA)

Rice husk is the hard protecting covering of grains of rice as shows in Figure 1.9, which is a by-product generally obtained from milling process of rice crop. The RHA is generated after burning the rice husk at temperatures between 500-700° C[85]. According to a RHA market study (2003), rice covers 1% of the earth's surface and is a primary source of food for billions of people. Globally, approximately 600 million tons of rice is produced each year. Thus, tons of rice husk are generated. On average 20% of the rice paddy harvest is husk, giving an annual total production of 120 million tons. For the transition from rice husk to RHA, the quantity of RHA generated is about 20% of the processed rice husk.

The RHA is highly porous and lightweight with a very high external surface area and contains around 90 - 95 wt% of amorphous biomass silica. For that reason, RHA is an excellent pozzolanic material for manufacture of cement, ceramic, refractory, insulator, roofing shingles, waterproofing chemicals, oil spill absorbent, flame retardants, etc.

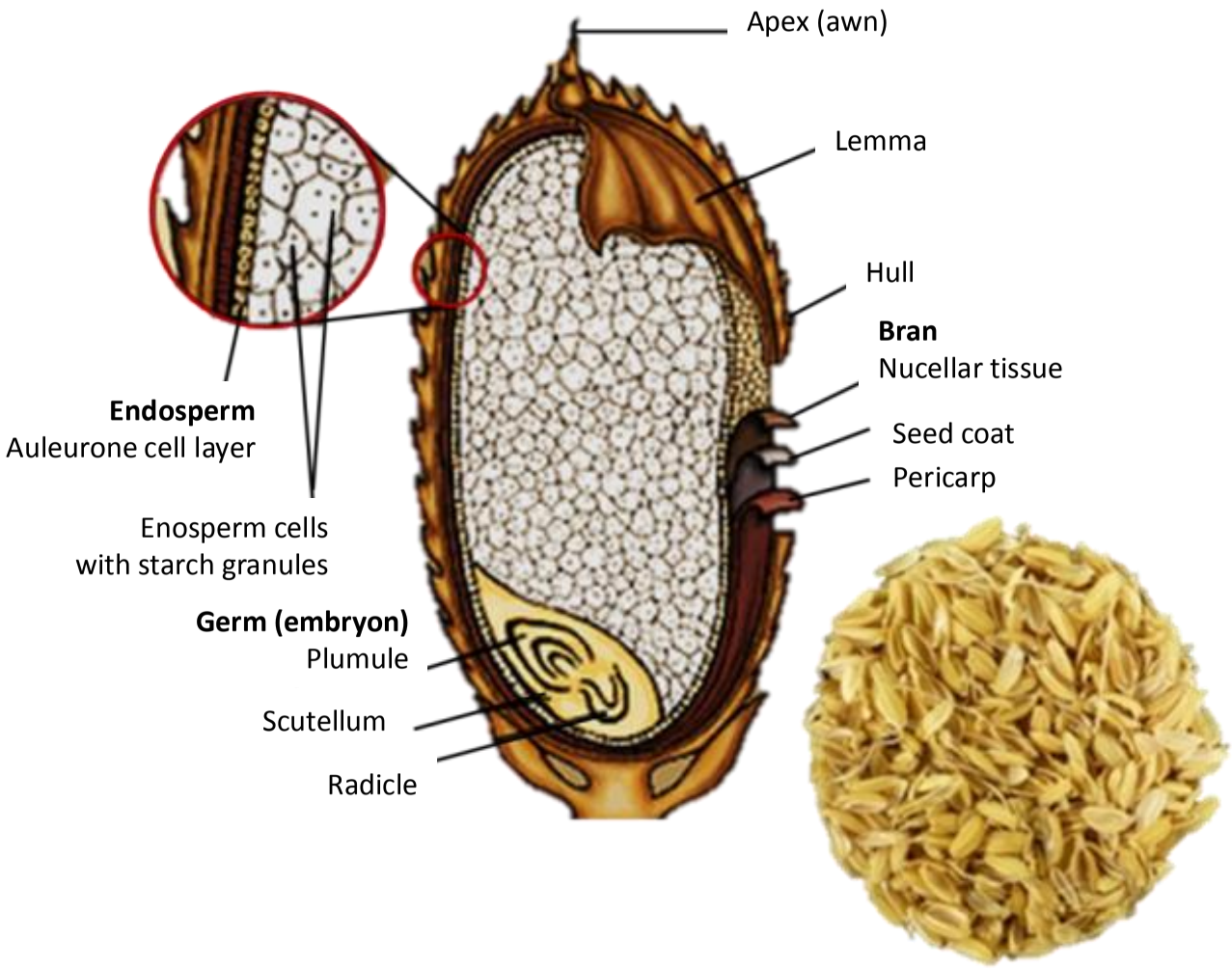

Fig. 1.9. Rice husk composition.

1.6. Scope of the present investigation

In the present study, several geopolymers were prepared by varying the molar concentration of Si, Al, Na and distilled H_2O through the ratios of Si/Al, Na/Si and H_2O/Na. The following nomenclature was used in order to describe the synthesized samples:

GP-[Si/Al]-[Na/Si]-[H_2O/Na]

where GP means geopolymer, [Si/Al], [Na/Si] and [H_2O/Na] is the molar ratio of the component in the geopolymer. For example, for GP-3-0.6-7 refers to a synthesized geopolymer with a molar ratio of [Si/Al] = 3, [Na/Si] = 0.6 and [H_2O/Na] = 7.

Extensive work on geopolymer research has been conducted so far. However, existing literature on the adsorption of heavy metals using geopolymers is very little, geopolymer adsorbents are challenging for study. Geopolymers could offer an alternative to remove heavy metals from wastewater via adsorption and become a new method for affecting both the environment and societies positively. Therefore, this work focused on a developing field that utilizes cheap and plentiful described geopolymer adsorbents composed of aluminosilicate of metakaolin (MK) which are excellent pozzolanic source materials to geopolymers. **Chapter 1** has presented a brief introduction of different methodologies of removing heavy metals from wastewater and polymers. Here are introduction of concepts of adsorption technology to pollutant and geopolymerization.

In **Chapter 2**, the effect of the amorphous silica derived from biomass rice husk (RH) in the alkaline activating solution on the properties was investigated in geopolymerization process, when metakaolin was used as the aluminum source from metakaolin (MK). With changing a molar ratio of Si/Al_2 = 3.0 and 10, the curing in the preparation of geopolymers was carried out at 85˚C, 100˚C and 200˚C. Viscoelastic properties of the geopolymer pastes including SiO_2 and Al_2O_3 components suggested that the alkaline activation was found in higher RH silica source. The mineralogical and microstructural characteristics of the cured products were evaluated to be amorphous aluminosilicate. In **Chapter 3**, Geopolymer adsorbents were prepared from silica and MK in different Al and Si components and the geopolymers were applied for removal of metal ions, Cs^+ and Pb^{2+}, from other heavy metal ions mixture. When geopolymer was optimized at Si/Al = 2 as adsorbent, targeting to Cs^+ and Pb^{2+} separation was observed. The binding behavior was well fitted to Langmuir model, which proved that the metakaolin-based geopolymer had multi-binding to adsorb ions. The effective adsorption was also observed independent of NaCl concentration for the Cs^+ and Pb^{2+}. This meant that the ion adsorption of geopolymers occurred under non-electrostatic mechanism. In **Chapter 4**, it is investigated that the geopolymer foam materials could obtained and applied as adsorbents for capture of cesium ions. Geopolymer foams showing cesium adsorption were prepared by condensing a mixture of MK and alkali solution at 100° C in the presence of RHA powder, and they showed effective adsorption of cesium.

In final **Chapter 5**, conclusion of this doctoral thesis is summarized.

1.7. Reference.

1. Srivastava NK, Majumder CB. Novel biofiltration methods for the treatment of heavy metals from industrial wastewater. *J. Hazard. Mater.* 2008;151(1):1–8.

2. Naseem R, Tahir S. Removal of Pb(II) from aqueous/acidic solutions by using bentonite as an adsorbent. *Water Res.* 2001;35(16):3982–3986.

3. Long H, Wu P, Yang L, Huang Z, Zhu N, Hu Z. Efficient removal of cesium from aqueous solution with vermiculite of enhanced adsorption property through surface modification by ethylamine. *J. Colloid Interface Sci.* 2014;428:295–301.

4. Richardson JF, Harker JH, Backhurst JR. *Chemical Engineering*. 5th ed. Elsevier; 2002.

5. Perić J, Trgo M, Vukojević Medvidović N. Removal of zinc, copper and lead by natural zeolite-a comparison of adsorption isotherms. *Water Res.* 2004;38(7):1893–9.

6. Inglezakis VJ, Loizidou MM, Grigoropoulou HP. Ion exchange studies on natural and modified zeolites and the concept of exchange site accessibility. *J. Colloid Interface Sci.* 2004;275(2):570–6.

7. Adamson AW. *Physical Chemistry of Surfaces*. (Wiley J, ed.).; 1982.

8. Zangwill A. *Physics at Surfaces*. Cambridge University Press; 1988.

9. Ramalho RS. *Introduction to Wastewater Treatment Processes*.; 1977:1977.

10. Hamdaoui O. Removal of copper(II) from aqueous phase by Purolite C100-MB cation exchange resin in fixed bed columns: modeling. *J. Hazard. Mater.* 2009;161(2-3):737–46.

11. Jusoh A, Su Shiung L, Ali N, Noor MJMM. A simulation study of the removal efficiency of granular activated carbon on cadmium and lead. *Desalination*. 2007;206(1-3):9–16.

12. Park HG, Kim TW, Chae MY, Yoo I-K. Activated carbon-containing alginate adsorbent for the simultaneous removal of heavy metals and toxic organics. *Process Biochem.* 2007;42(10):1371–1377.

13. Üçer A, Uyanik A, Aygün ŞF. Adsorption of Cu(II), Cd(II), Zn(II), Mn(II) and Fe(III) ions by tannic acid immobilised activated carbon. *Sep. Purif. Technol.* 2006;47(3):113–118.

14. Yanagisawa H, Matsumoto Y, Machida M. Adsorption of Zn(II) and Cd(II) ions onto magnesium and activated carbon composite in aqueous solution. *Appl. Surf. Sci.* 2010;256(6):1619–1623.

15. Ahn CK, Park D, Woo SH, Park JM. Removal of cationic heavy metal from aqueous solution by activated carbon impregnated with anionic surfactants. *J. Hazard. Mater.* 2009;164(2-3):1130–6.

16. Dias JM, Alvim-Ferraz MCM, Almeida MF, Rivera-Utrilla J, Sánchez-Polo M. Waste materials for activated carbon preparation and its use in aqueous-phase treatment: a review. *J. Environ. Manage.* 2007;85(4):833–46.

17. Kongsuwan A, Patnukao P, Pavasant P. Binary component sorption of Cu(II) and Pb(II) with activated carbon from Eucalyptus camaldulensis Dehn bark. *J. Ind. Eng. Chem.* 2009;15(4):465–470.

18. Bhattacharyya KG, Gupta S Sen. Adsorption of a few heavy metals on natural and modified kaolinite and montmorillonite: a review. *Adv. Colloid Interface Sci.* 2008;140(2):114–31.

19. Sud D, Mahajan G, Kaur MP. Agricultural waste material as potential adsorbent for sequestering heavy metal ions from aqueous solutions - a review. *Bioresour. Technol.* 2008;99(14):6017–27.

20. Wan Ngah WS, Hanafiah MAKM. Removal of heavy metal ions from wastewater by chemically modified plant wastes as adsorbents: a review. *Bioresour. Technol.* 2008;99(10):3935–48.

21. Babel S. Low-cost adsorbents for heavy metals uptake from contaminated water: a review. *J. Hazard. Mater.* 2003;97(1-3):219–243. Available at: http://www.sciencedirect.com/science/article/pii/S0304389402002637. Accessed May 28, 2014.

22. Sheng G, Wang S, Hu J, et al. Adsorption of Pb(II) on diatomite as affected via aqueous solution chemistry and temperature. *Colloids Surfaces A Physicochem. Eng. Asp.* 2009;339(1-3):159–166.

23. Köhler SJ, Cubillas P, Rodríguez-Blanco JD, Bauer C, Prieto M. Removal of cadmium from wastewaters by aragonite shells and the influence of other divalent cations. *Environ. Sci. Technol.* 2007;41(1):112–8.

24. Apiratikul R, Pavasant P. Sorption of Cu2+, Cd2+, and Pb2+ using modified zeolite from coal fly ash. *Chem. Eng. J.* 2008;144(2):245–258.

25. ALJLIL S, ALSEWAILEM F. Saudi Arabian clays for lead removal in wastewater. *Appl. Clay Sci.* 2009;42(3-4):671–674.

26. Gu X, Evans LJ. Surface complexation modelling of Cd(II), Cu(II), Ni(II), Pb(II) and Zn(II) adsorption onto kaolinite. *Geochim. Cosmochim. Acta*. 2008;72(2):267–276.

27. LIU Z, ZHOU L, WEI P, ZENG K, WEN C, LAN H. Competitive adsorption of heavy metal ions on peat. *J. China Univ. Min. Technol.* 2008;18(2):255–260.

28. Jiang M, Jin X, Lu X-Q, Chen Z. Adsorption of Pb(II), Cd(II), Ni(II) and Cu(II) onto natural kaolinite clay. *Desalination*. 2010;252(1-3):33–39.

29. Agouborde L, Navia R. Heavy metals retention capacity of a non-conventional sorbent developed from a mixture of industrial and agricultural wastes. *J. Hazard. Mater.* 2009;167(1-3):536–44.

30. Aman T, Kazi AA, Sabri MU, Bano Q. Potato peels as solid waste for the removal of heavy metal copper(II) from waste water/industrial effluent. *Colloids Surf. B. Biointerfaces*. 2008;63(1):116–21.

31. Kaczala F, Marques M, Hogland W. Lead and vanadium removal from a real industrial wastewater by gravitational settling/sedimentation and sorption onto Pinus sylvestris sawdust. *Bioresour. Technol.* 2009;100(1):235–43.

32. Saeed A, Iqbal M, Akhtar MW. Removal and recovery of lead(II) from single and multimetal (Cd, Cu, Ni, Zn) solutions by crop milling waste (black gram husk). *J. Hazard. Mater.* 2005;117(1):65–73.

33. Amuda OS, Adelowo FE, Ologunde MO. Kinetics and equilibrium studies of adsorption of chromium(VI) ion from industrial wastewater using Chrysophyllum albidum (Sapotaceae) seed shells. *Colloids Surf. B. Biointerfaces*. 2009;68(2):184–92.

34. Oliveira LS, Franca AS, Alves TM, Rocha SDF. Evaluation of untreated coffee husks as potential biosorbents for treatment of dye contaminated waters. *J. Hazard. Mater.* 2008;155(3):507–12.

35. Mata YN, Blázquez ML, Ballester A, González F, Muñoz JA. Sugar-beet pulp pectin gels as biosorbent for heavy metals: Preparation and determination of biosorption and desorption characteristics. *Chem. Eng. J.* 2009;150(2-3):289–301.

36. Schiewer S, Patil SB. Modeling the effect of pH on biosorption of heavy metals by citrus peels. *J. Hazard. Mater.* 2008;157(1):8–17.

37. Apiratikul R, Pavasant P. Batch and column studies of biosorption of heavy metals by Caulerpa lentillifera. *Bioresour. Technol.* 2008;99(8):2766–77.

38. Li L, Wang S, Zhu Z. Geopolymeric adsorbents from fly ash for dye removal from aqueous solution. *J. Colloid Interface Sci.* 2006;300(1):52–9.

39. Wang S, Li L, Zhu ZH. Solid-state conversion of fly ash to effective adsorbents for Cu removal from wastewater. *J. Hazard. Mater.* 2007;139(2):254–9.

40. Yousef RI, El-Eswed B, Alshaaer M, Khalili F, Khoury H. The influence of using Jordanian natural zeolite on the adsorption, physical, and mechanical properties of geopolymers products. *J. Hazard. Mater.* 2009;165(1-3):379–87.

41. He J, Zhang G, Asce M, Hou S, Cai CS. Geopolymer-Based Smart Adhesives for Infrastructure Health Monitoring : Concept and Feasibility. *J. Mater. Civ. Eng.* 2011;23(February):100–109.

42. Cheng TW, Lee ML, Ko MS, Ueng TH, Yang SF. The heavy metal adsorption characteristics on metakaolin-based geopolymer. *Appl. Clay Sci.* 2012;56:90–96.

43. El-Eswed B, Alshaaer M, Ibrahim Yousef R, Hamadneh I, Khalili F. Adsorption of Cu(II), Ni(II), Zn(II), Cd(II) and Pb(II) onto Kaolin/Zeolite Based- Geopolymers. *Adv. Mater. Phys. Chem.* 2012;02(04):119–125.

44. López FJ, Sugita S, Takaomi K. Cesium-adsorbent Geopolymer Foams Based on Silica from Rice Husk and Metakaolin. *Chem. Lett.* 2014;43(1):128–130.

45. Davidovits J. Geopolymers and geopolymeric materials. *J. Therm. Anal. Calorim.* 1989;35:429–441.

46. Lyon RE, Balaguru PN, Foden A, Sorathia U, Davidovits J, Davidovics M. Fire-resistant Aluminosilicate Composites. *Fire Mater.* 1997;21(2):67–73.

47. Giancaspro J, Asce M, Balaguru PN, Lyon RE. Use of Inorganic Polymer to Improve the Fire Response of Balsa Sandwich Structures. *J. Mater. Civ. Eng.* 2006;18(June):390–397.

48. Barbosa VFF, MacKenzie KJD. Thermal behaviour of inorganic geopolymers and composites derived from sodium polysialate. *Mater. Res. Bull.* 2003;38(2):319–331.

49. Balaguru P. *Geopolymer for Protective Coating of Transportation Infrastructures*.; 1998.

50. Zhang S, Gong K, Lu J. Novel modification method for inorganic geopolymer by using water soluble organic polymers. *Mater. Lett.* 2004;58(7-8):1292–1296.

51. Li Z, Zhang Y, Zhou X. Short Fiber Reinforced Geopolymer Composites Manufactured by Extrusion. *J. Mater. Civ. Eng.* 2005;17(December):624–631.

52. Allahverdi ALI, Mehrpour K, Kani EN. Investigating the possibility of utilizing pumice-type natural pozzonal in production of geopolymer cement. *Ceram. - Silikaty*. 2008;52(1):16–23.

53. Verdolotti L, Iannace S, Lavorgna M, Lamanna R. Geopolymerization reaction to consolidate incoherent pozzolanic soil. *J. Mater. Sci.* 2007;43(3):865–873.

54. Xu H, Van Deventer JSJ. The geopolymerisation of alumino-silicate minerals. *Int. J. Miner. Process.* 2000;59(3):247–266.

55. Davidovits J, Quentin S. GEOPOLYMERS Inorganic polymerie new materials. 1991;37:1633–1656.

56. Duxson P, Fernández-Jiménez a., Provis JL, Lukey GC, Palomo a., Deventer JSJ. Geopolymer technology: the current state of the art. *J. Mater. Sci.* 2006;42(9):2917–2933.

57. Rattanasak U, Chindaprasirt P. Influence of NaOH solution on the synthesis of fly ash geopolymer. *Miner. Eng.* 2009;22(12):1073–1078.

58. Yunsheng Z, We S, Zuquan J, Hongfa Y, Yantao J. In situ observing the hydration process of K-PSS geopolymeric cement with environment scanning electron microscopy. *Mater. Lett.* 2007;61(7):1552–1557.

59. Van Jaarsveld JG., van Deventer JS., Lukey G. The effect of composition and temperature on the properties of fly ash- and kaolinite-based geopolymers. *Chem. Eng. J.* 2002;89(1-3):63–73.

60. Swanepoel JC, Strydom C a. Utilisation of fly ash in a geopolymeric material. *Appl. Geochemistry*. 2002;17(8):1143–1148.

61. Liu C, Kong D, Guo H. The morphology control of zeolite ZSM-5 by regulating the polymerization degree of silicon and aluminum sources. *Microporous Mesoporous Mater.* 2014;193:61–68.

62. Davidovits J. *Geopolymer Chemistry and Applications 3 rd edition*. 3rd ed. San Quintín: Insttut Géopolymère; 2011.

63. Palomo A, Grutzeck MW, Blanco MT. Alkali-activated fly ashes A cement for the future. *Cem. Concr. Res.* 1999;29:1323–1329.

64. Provis JL, Lukey G., van Deventer JS. Do Geopolymers Actually Contain Nanocrystalline Zeolites? A Reexamination of Existing Results. *Chem. Mater.* 2005;17:3075–3085.

65. Xu X, Yang W, Liu J, Lin L. Synthesis of NaA zeolite membrane by microwave heating. *Sep. Purif. Technol.* 2001;25(1-3):241–249.

66. Phair JW, Van Deventer JSJ, Smith JD. Mechanism of Polysialation in the Incorporation of Zirconia into Fly Ash-Based Geopolymers. *Ind. Eng. Chem. Res.* 2000;39(8):2925–2934.

67. Singh PS, Bastow TIM, Trigg M, Mdc CS. Structural studies of geopolymers by 29 Si and 27 Al MAS-NMR. 2005;0:3951–3961.

68. Cioffi R, Maffucci L, Santoro L. Optimization of geopolymer synthesis by calcination and polycondensation of a kaolinitic residue. *Resour. Conserv. Recycl.* 2003;40(1):27–38.

69. Komnitsas K, Zaharaki D, Perdikatsis V. Geopolymerisation of low calcium ferronickel slags. *J. Mater. Sci.* 2006;42(9):3073–3082.

70. Dombrowski K, Buchwald a., Weil M. The influence of calcium content on the structure and thermal performance of fly ash based geopolymers. *J. Mater. Sci.* 2006;42(9):3033–3043.

71. Riessen A. Thermo-mechanical and microstructural characterisation of sodium-poly(sialate-siloxo) (Na-PSS) geopolymers. *J. Mater. Sci.* 2006;42(9):3117–3123.

72. Komnitsas K, Zaharaki D. Geopolymerisation: A review and prospects for the minerals industry. *Miner. Eng.* 2007;20(14):1261–1277.

73. Sofi M, van Deventer JSJ, Mendis P a., Lukey GC. Engineering properties of inorganic polymer concretes (IPCs). *Cem. Concr. Res.* 2007;37(2):251–257.

74. Goretta KC, Chen N, Gutierrez-Mora F, Routbort JL, Lukey GC, van Deventer JSJ. Solid-particle erosion of a geopolymer containing fly ash and blast-furnace slag. *Wear*. 2004;256(7-8):714–719.

75. Jaarsveld JGSVAN, Deventer JSJVAN, Lorenzeni L. The potential use of geopolymeric materials to immobilise toxic metals : part I . theory and applications. 1997;10(7):659–669.

76. Van Jaarsveld JGS, van Deventer JSJ. Effect of the Alkali Metal Activator on the Properties of Fly Ash-Based Geopolymers. *Ind. Eng. Chem. Res.* 1999;38(10):3932–3941.

77. Xu JZ, Zhou YL, Chang Q, Qu HQ. Study on the factors of affecting the immobilization of heavy metals in fly ash-based geopolymers. *Mater. Lett.* 2006;60(6):820–822.

78. Matusik J, Gaweł A, Bahranowski K. Grafting of methanol in dickite and intercalation of hexylamine.

79. Zhang Y, Liu Q, Xiang J, Zhang S, Frost RL. Insight into morphology and structure of different particle sized kaolinites with same origin. *J. Colloid Interface Sci.* 2014;426:99–106.

80. Li Z, Bowman RS. Retention of inorganic oxyanions by organo-kaolinite. *Water Res.* 2001;35(16):3771–6.

81. Xu H, Van Deventer JSJ. Microstructural characterisation of geopolymers synthesised from kaolinite/stilbite mixtures using XRD, MAS-NMR, SEM/EDX, TEM/EDX, and HREM. *Cem. Concr. Res.* 2002;32(11):1705–1716.

82. Salvador S. Pozzolanic properties of flash-calcined kaolinite: a comparative study with soak-calcined products. 1995;25(1):102–112.

83. Sabir B., Wild S, Bai J. Metakaolin and calcined clays as pozzolans for concrete: a review. *Cem. Concr. Compos.* 2001;23(6):441–454.

84. Barbosa VFF, MacKenzie KJD. Synthesis and thermal behaviour of potassium sialate geopolymers. *Mater. Lett.* 2003;57(9-10):1477–1482.

85. Chakraverty A, Mishra P, Banerjee HD. Investigation of combustion of raw and acid-leached rice husk for production of pure amorphous white silica. *J. Mater. Sci.* 1988;23:21–24.

Chapter 2

Geopolymers Using Rice Husk Silica and Metakaolin Derivatives; Preparation and Their Characteristics.

2.1 Introduction.

Geopolymerization is an effective manner to process and reuse silicates, aluminates or aluminosilicates in mineral waste. It is known that geopolymers are alkaline activated aluminosilicates consisting of reactive species of SiO_2 and Al_2O_3 to produce high-strength materials that can effectively immobilize other industrial by-products, and even hazardous waste. Generally, the formula of the geopolymers is $M_n(-(Si-O_2)_z-Al-O)_n \cdot wH_2O$, where M is an alkaline cation (Na, K or Ca), z is generally assigned a value of 1, 2 or 3 and n is the degree of polymerization[1]. Geopolymers are interesting materials formed by polycondensation of the silicon and aluminum species resulting from the dissolution of their raw materials found in fly ash, slag, MK in alkaline solution condition[2]. Usually, the geopolycondenzation depends of Si/Al ratio and alkali concentration[3,4]. Geopolymerization is affected by the reactive precursor, meaning that OH^- concentration and curing conditions finally produce three-dimensional networks that comprise geopolymer matrices at different time and temperature[5]. Therefore, the advantage is the proven durability and erosion resistance of both ancient mortars and cements and modern geopolymer cements. It was known that a great number of minerals-industrial wastes were studied as raw

materials for geopolymer synthesis, including pozzolana[6], natural aluminosilicate minerals, MK, fly ash, granulated blast furnace slag, fly ash and kaolinite mixture, red mud and MK mixture[3,7–10]. More importantly, the starting raw materials play a significant role in the geopolymer reaction and affect the mechanical properties and microstructure of the final geopolymericproducts[11,12]. It would be expected that silica from of rice husk (RH) is an excellent pozzolanic material, but that has not been extensively studied in geopolymerization. RH silica can be generate by the combustion process of RH[13], itself is biomass and to be an issue for sustainability environment, due to its abundant amount and capability to resist natural degradation. RH silica therefore is an alternative material with good pozzolanic reactivity, to be included in the geopolymer mixture to complete the ratio of modulus of Si/Al. In the present study, the effect of the RH silica was determined on the resultant geopolymers as a function of curing time and temperature. It was investigated that the rheometry properties of the geopolymer pastes and properties of resultant geopolymers were compared at different Si/Al ratios at different cure temperature in addition with their bulk characteristics. Since such biomass resource was attractively interesting in point of view of sustainability, this paper focused on the detail in the geopolymerization.

2.2 Experimental

2.2.1 Materials

Obtaining MK was carry out by dehydroxylation of kaolinite at 750° C by 20 h according to reference[14,15]. The chemical composition of MK was measured by XRF for 52 % of SiO_2 and 42.1 % of Al_2O_3. The surface area of MK calculated from BET method was 11.5 m^2/g.

2.2.2 Synthesis and properties of RHA.

Rice husk obtained from Niigata, Japan, was thoroughly wet cleaned and dried. The paddy husk was leached with HCl at 5 M for one night. After leaching, the husk was thoroughly washed with distilled water and then dried. Then, about 30 g of the acid-treated husk sample were taken in alumina crucibles, placed in an electric muffle furnace and burned at 700° C for 4 h. Figure 2.1 shows the white ash obtained after the thermal treatment. XRF of RHA revealed a 99.5 % of SiO_2 and the surface area by BET method was 207.5 m^2/g, which is shown in table 2.1.

Table 2.1. Chemical composition and properties of RHA.

Composition [%]	SiO_2	Al_2O_3	CaO	MgO	Na_2O	K_2O	Fe_2O_3	BET
RHA	99.5	0	0.2	0.1	0.0	0.0	0	207.5 m2/g

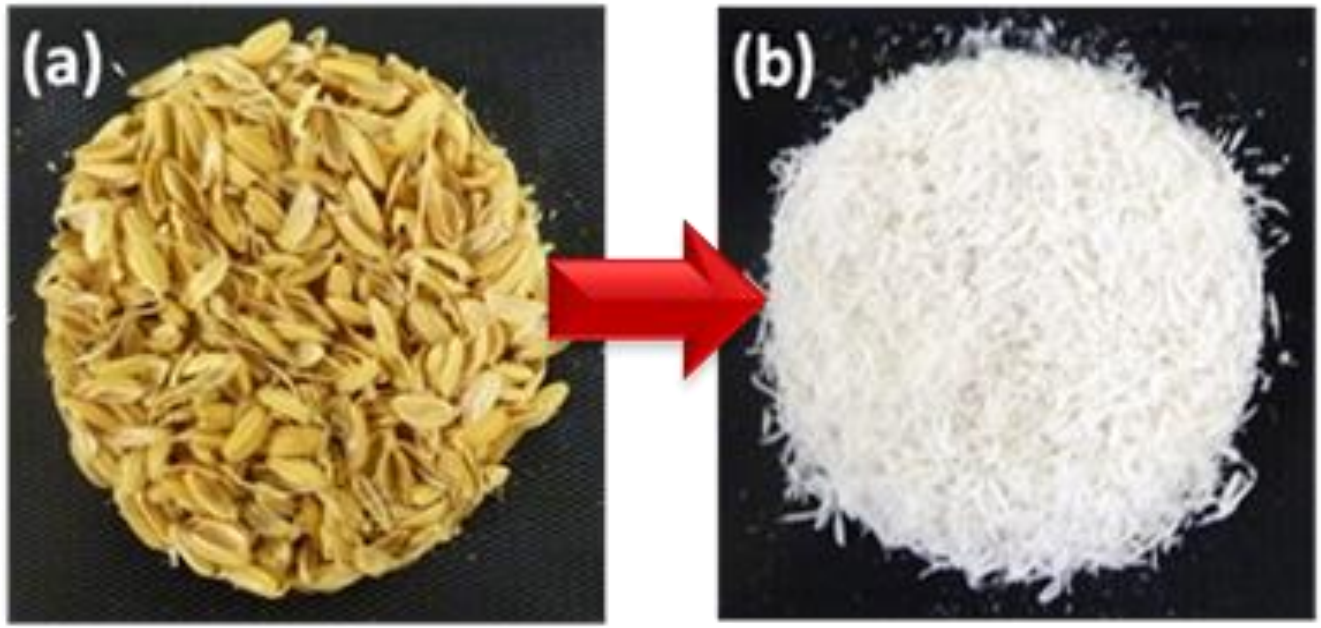

Fig. 2.1. RHA obtained after burning rice husk at 700° C for 4 h.

2.2.3 Preparation of Geopolymer

Geopolymers were prepared by changing a molar ratio of Si/Al = 3 and 10. For NaOH, Na_2SiO_3 and H_2O molar ratio of Na_2O/SiO_2 = 0.25 and H_2O/Na = 10 were used. Geopolymers was named GP-3-0.25-10 and GP-10-0.25-10, respectively. The preparation procedure is as followed as described in Figure 2.2. The powders of RH silica were mixed with NaOH solution until dissolution. Then, MK powders were added and mixed together for 15 min in the silica solution. The paste samples were cast in plastic molds with a diameter of 20 mm and height of 40 mm. The curing time for preparation of geopolymers was carried out at 85°, 100° and 200° C in a conventional oven at open mold. Before the curing process, rheological measurements of the paste samples were performed using a controlled stress rheometer (Anton PaarPhysica MCR 301 Rheometer), as operated in controlled strain mode. The geopolymer paste was prepared manually outside the rheometer and then introduced into the rheometer disk after mixing. Transferring the geopolymer to the measurement cell generates residual stresses, when the sample was prior to each rheological measurement. This was done before each test by applying a strain at frequency of 1 Hz. Characterization of the geopolymers was obtained by infrared spectroscopy (FT-IR), X-ray diffraction (XRD) and scanning electron microscope (SEM).

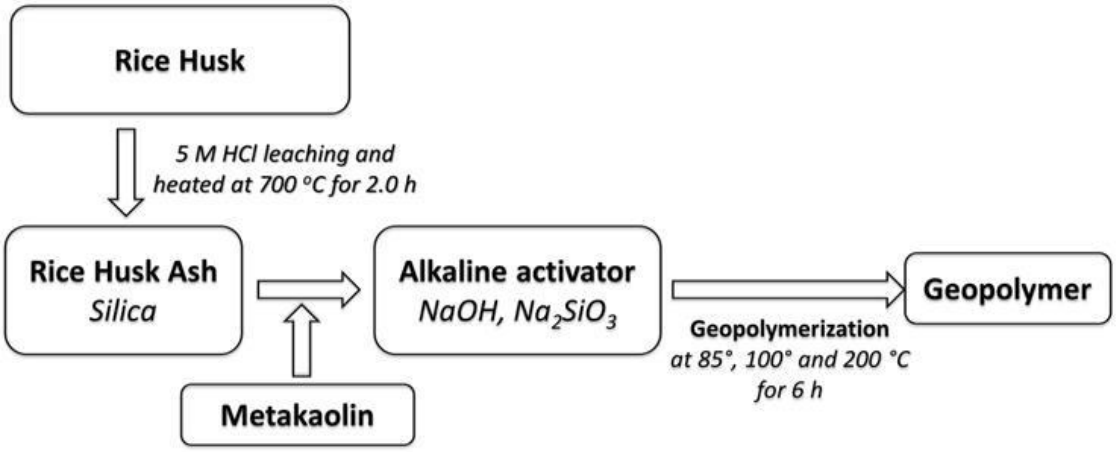

Fig. 2.2. Protocol of geopolimerization synthesis.

2.3 Results and Discussion

Figure 2.2. presents synthesis protocol of RH silica-MK geopolymerization. In this process, the RH silica and MK were produced by sintered RH and kaolin at 700° and 750° C, respectively, before the provided. Figure 2.3. shows the strain sweep at a frequency of 1 Hz for raw material activated by NaOH and geopolymer paste with a satisfactory repeatability. It was observed in the viscous elastic rheometer that the deformation of the geopolymers pastes (a) was higher than that of RH silica and MK (b). It was understanding that the linear viscoelasticity region was due to nondestructive to the geopolymerization of the silica-alumina component in the activated paste, when a critical strain γ_C was applied. Strain was generally taken as the strain value at the storage modulus equal to 90 % of the plateau modulus. In both cases for GP-3-0.25-10 and GP-10-0.25-10, the elastic modulus (G') came to be higher than that of viscous modulus (G"). That meant that the paste was considered in the gelation for solid.

When comparison made between the paste of GP-3-0.25-10 and GP-10-0.25-10, high values of G' and G" for geopolymers pastes were observed, indicating that the geopolymerization in the activator condition was easily occur at the point of G"/G' = 1, GP-3-0.25-10 containing higher alumina and higher strain. This means that the high MK content was better for the polycondensation reaction.

Figure 2.4 show time curves of G' and G" at different temperature. It was also observed at fixed temperature of 60°, 85° and 100° for GP-3-0.25-10 and GP-10-0.25-10. The both G' and G" were increased with increasing time and then became to be constant at about 250 seconds. The comparison between GP-3-0.25-10 and GP-10-0.25-10 meant that the cure ability of the activated paste was higher in GP-10-0.25-10. The time curves suggested that the curing was finished at about 2 min heating. But, the GP-3-0.25-10 increased the G' and G" values near 200-250 seconds and then was cured in the geopolymer solidified. Due to that the polycondensation reaction occurs, the geopolymer paste loses viscosity, while the paste became a solid material, the elastic modulus became constant at the longer time. This change was exactly observed after 250 s for GP-3-0.25-10 at 60° C and 210 s for GP-3-0.25-10 at 85° C and 100° C. At a high amount of Al_2O_3 for GP-3-0.25-10, it was less to be on geopolymerization. However, the GP-10-0.25-10 registered a constant modulus G' and G" for all the cases due to with a high content of RH silica on the geopolymer pastes which made a very elastic and viscous material even after 250 s.

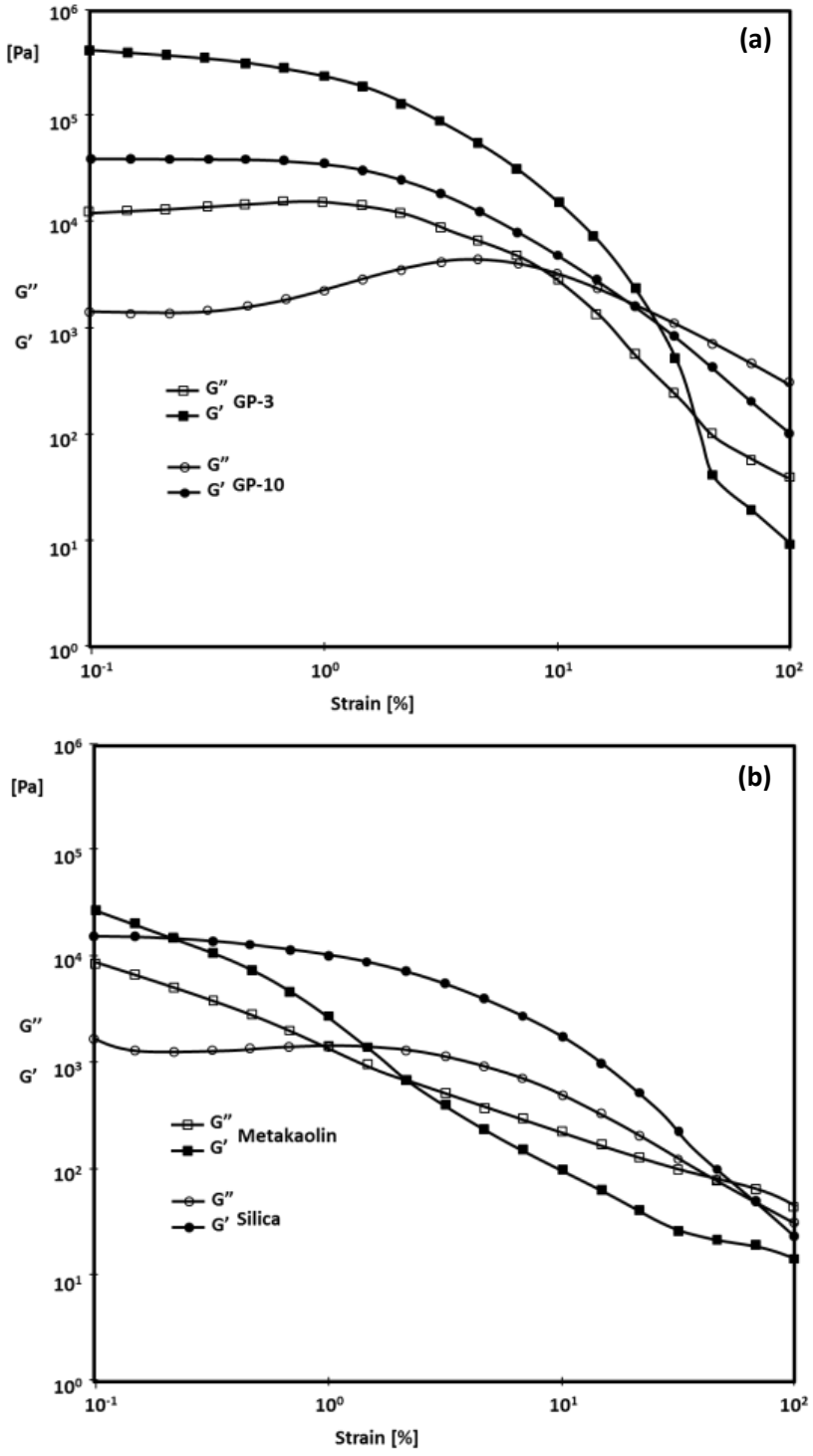

Fig. 2.3. Strain sweep test for (a) geopolymer paste of GP-3-0.25-10 and GP-10-0.25-10 at 25 °C, and (b); RHA and MK activated by NaOH.

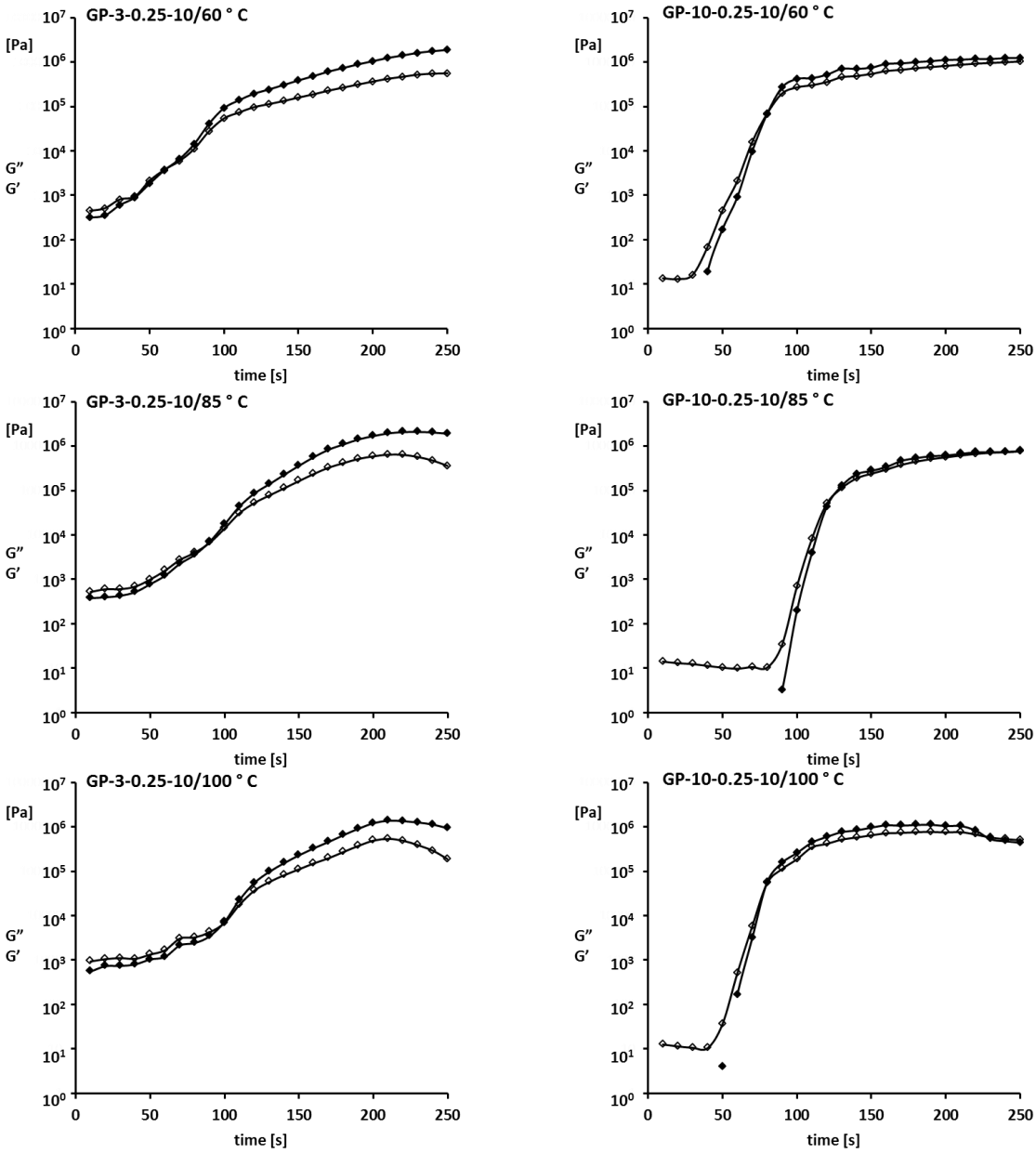

Fig. 2.4. The G’ and G” as a function of time and maintaining a constant temperature at 60˚C, 85˚C and 100˚C for GP-3-0.25-10 and GP-10-0.25-10 [◆for elastic modulus (G’) and ◇ for viscous modulus (G’’)].

Figure 2.5 shows viscosity of the pastes of GP-3-0.25-10 and GP-10-0.25-10 at different temperature. It was noticed that the viscoelasticity of the paste decreased, when the temperature was high. The resultant viscosity of the GP-10-0.25-10 was higher than that of GP-3-0.25-10, due to the increment of the SiO_2 in geopolymer composition resulted in a decrease of the viscosity of the pastes. After polycondensation reaction for GP-3-0.25-10 and GP-10-0.25-10, the microstructures of geopolymers at different curing temperature were observed.

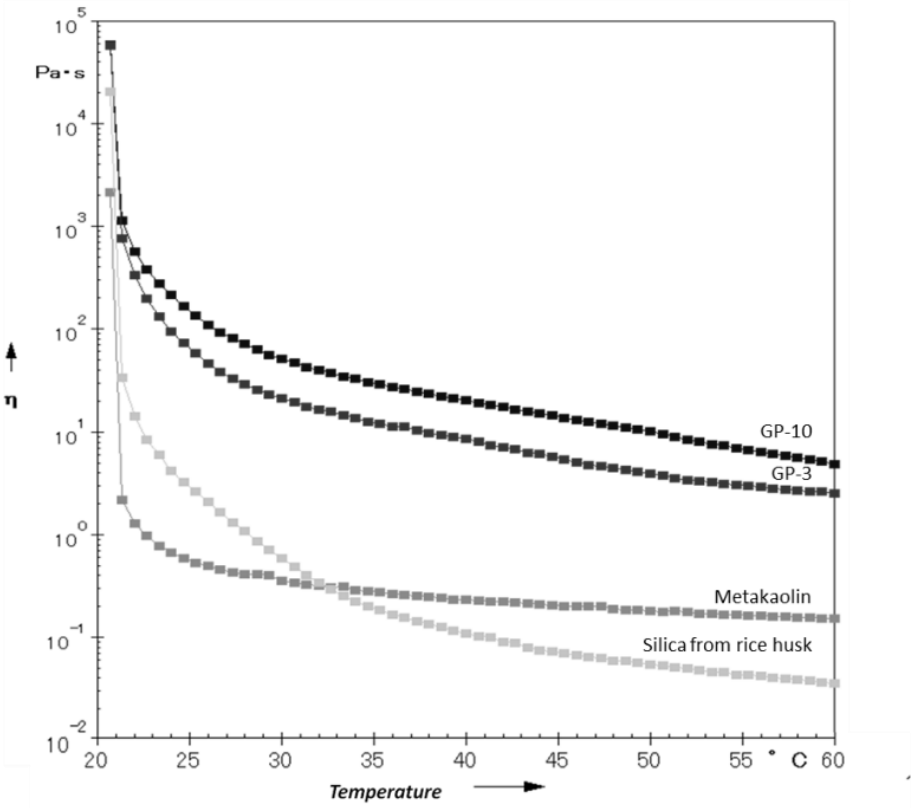

Fig. 2.5. Viscosity test for silica from rice husk, MK activated by NaOH and geopolymer paste of GP-3-0.25-10 and GP-10-0.25-10 from 20° C to 60° C.

Figure 2.6 shows microscope picture for the resultant geopolymers. The pictures showed the formation of the heterogeneous matrix after the polycondensation of raw material. It was seen that the geopolymers of the GP-3-0.25-10 became to be more porosity matrix. Their porosities of the geopolymers decreased at the GP-10-0.25-10 containing higher RH silica contents. It was seen that with the increment of the temperature, changing into a homogeneous phase was found in the geopolymer matrix, which was condensed at 200° C of the geopolymer matrix.

The XRD patters of the geopolymers of GP-3-0.25-10 and GP-10-0.25-10 at different curing temperature are shown in Figure 2.7. It was seen that the peak shift toward higher 2θ side was significant in the cases of GP-3-0.25-10. This meant that the reconstruction of silica-alumina order in the paste was highly observed at the polycondensed GP-3-0.25-10. This was strongly demonstrated geopolymerization with the amorphous nature of the samples. In addition with the XRD results, the alteration and restructuring of materials during geopolymerization were also suggested in the diffraction pattern by the marked shift in the scattering diffraction peak for each sample. When the starting materials were activated with an alkaline solution, the scattering diffraction peak shifted from ~20° to ~25°-28° in 2θ. This suggested that the local bonding environment was changed during the geopolymerization process[16]. Apparently, an increase of the temperature from 85° C to 200° C, no influence of the amorphous structure of the geopolymers was observed.

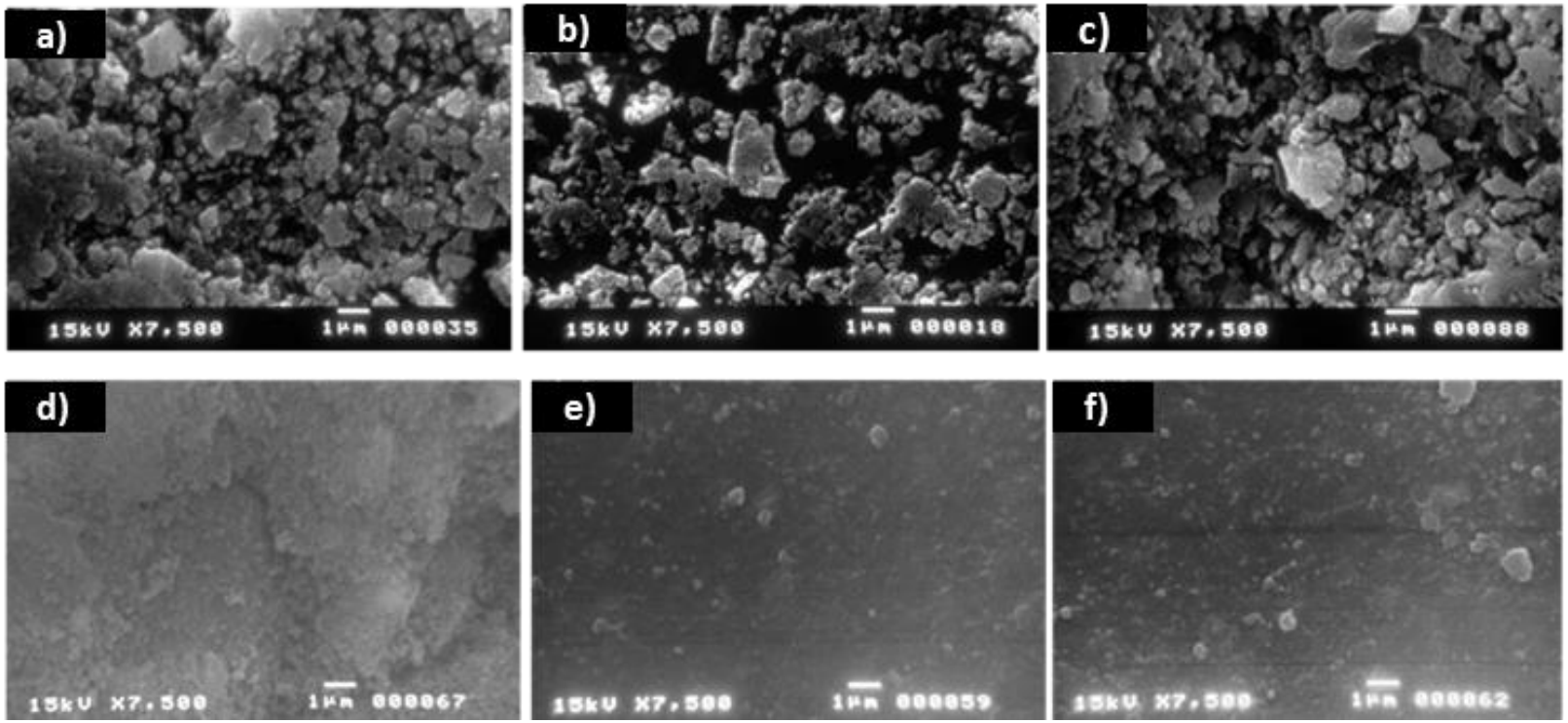

Fig. 2.6. SEM imagines of (a) GP-3-0.25-10 at 85° C; (b) GP-3-0.25-10 at 100° C; (c) GP-3-0.25-10 at 200° C; (d) GP-10-0.25-10 at 85° C; (e) GP-10-0.25-10 at 100°C and (f) GP-10-0.25-10 at 200° C.

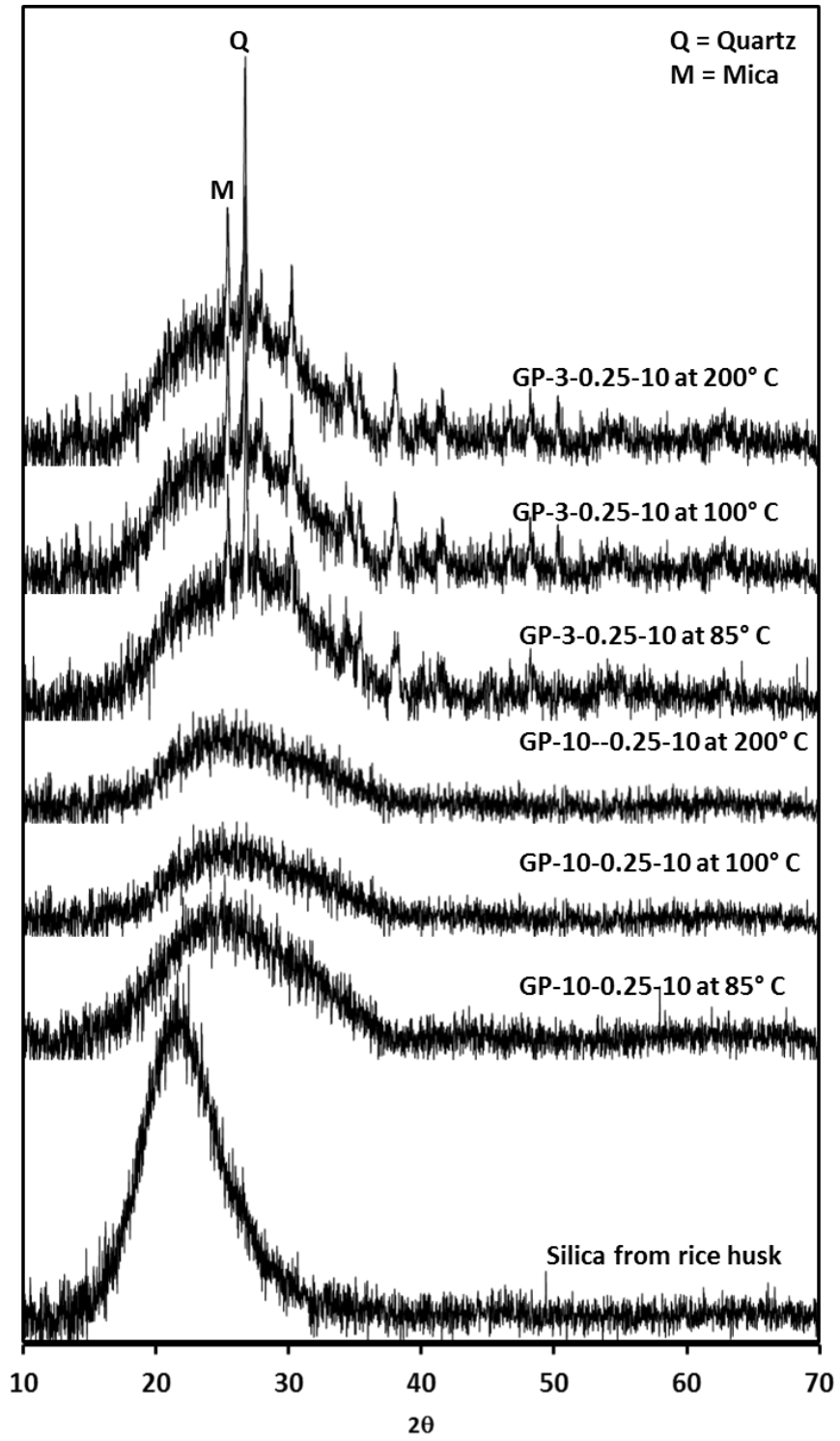

Fig. 2.7. X-ray diffraction of geopolymers synthetized by alkali activation of silica from RH and MK different curing time.

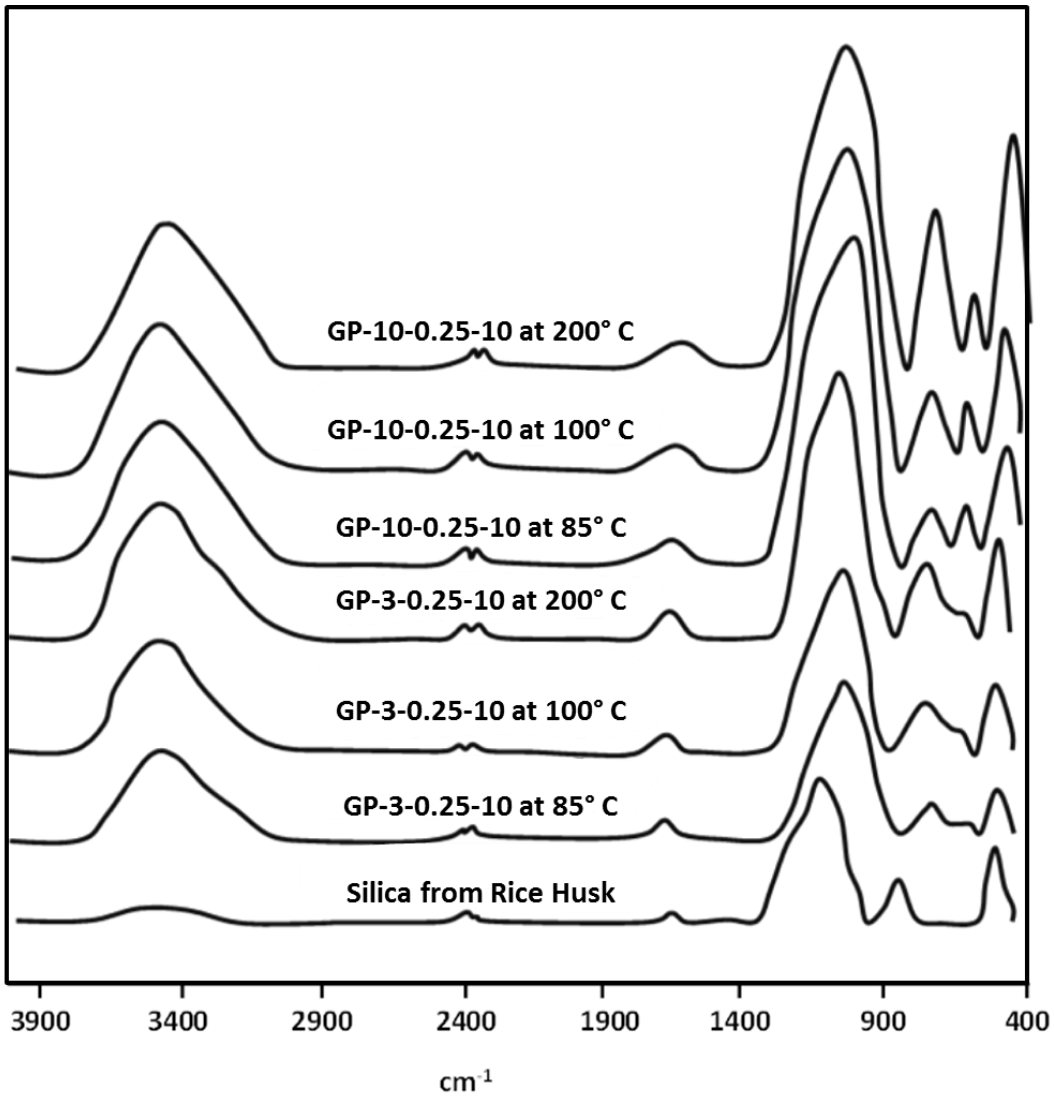

Fig. 2.8. Infrared spectra of geopolymers synthetized by alkali activation of RHA and MK at different curing time.

The data suggested that the silica/alumina component was affected to the reconstruction. In order to confirm this from chemical reaction of RH silica and MK we measured FT-IR spectra of the resultant GP-3-0.25-10 and GP-10-0.25-10. Figure 2.8 shows the infrared spectra of the geopolymer matrixes. The band around 460 cm^{-1} was related to Al–O and Si–O in plane and bending modes, 730 cm^{-1} with octahedral Al and 820 cm^{-1} with tetrahedral Al–O stretching and, the peak 1030 cm^{-1} was assigned with asymmetric Si-O-Al stretching[17]. The change in the intensity of the IR peaks was associated with the structural reorganization by the geopolymerization of RH silica and MK. In the geopolymer samples prepared using the RH silica, there was an increase and broaden in the IR intensity of IR peaks indicating higher polymerization, when the content of the RH silica was high. The IR peak around 1030 cm^{-1} meant that overlapping of the IR peaks related to SiQ_n (n = 0-4) structural units[18] was caused and became broaden, especially a higher temperature. In addition, the spectral data has broadening peak at 3400 cm^{-1} for OH stretching of Si-OH and Al-OH. It was apparent that the GP-10-0.25-10 system contained broadening tendency on the OH stretching peak. This meant that higher RH silica content easily occurred in the geopolymerization with MK.

2.4. Conclusion

Based on the result of these analyses, it could be concluded that silica obtained from RH combustion at 700° C became to be raw material for geopolymers and significantly contributed to the formation of geopolymer matrix with MK. The presence of the RH silica was an important during the geopolymerization reaction due to sodium

hydroxide activation. The evolution of the viscoelastic parameters of the geopolymers GP-3-0.25-10 and GP-10-0.25-10 were performed by dynamic rheology method for pastes. In general, the elastic modulus quickly exceeded the viscous modulus regardless of the geopolymer studied, indicating that both materials was on the process of solidified geopolymerization having reconstructed Si and Al species.

2.5. Reference

1. Davidovits J. Geopolymers and geopolymeric materials. *J. Therm. Anal. Calorim.* 1989;35:429–441.

2. Fernández-Jiménez a., Palomo a. Composition and microstructure of alkali activated fly ash binder: Effect of the activator. *Cem. Concr. Res.* 2005;35(10):1984–1992.

3. Xu H, Van Deventer JSJ. The geopolymerisation of alumino-silicate minerals. *Int. J. Miner. Process.* 2000;59(3):247–266.

4. Xu H, Van Deventer JSJ. Geopolymerisation of multiple minerals. *Miner. Eng.* 2002;15(12):1131–1139.

5. Rovnaník P. Effect of curing temperature on the development of hard structure of metakaolin-based geopolymer. *Constr. Build. Mater.* 2010;24(7):1176–1183.

6. Allahverdi ALI, Mehrpour K, Kani EN. Investigating the possibility of utilizing pumice-type natural pozzonal in production of geopolymer cement. *Ceram. - Silikaty*. 2008;52(1):16–23.

7. Davidovits J, Quentin S. GEOPOLYMERS Inorganic polymerie new materials. 1991;37:1633–1656.

8. Duxson P, Fernández-Jiménez a., Provis JL, Lukey GC, Palomo a., Deventer JSJ. Geopolymer technology: the current state of the art. *J. Mater. Sci.* 2006;42(9):2917–2933.

9. He J, Zhang G, Asce M, Hou S, Cai CS. Geopolymer-Based Smart Adhesives for Infrastructure Health Monitoring : Concept and Feasibility. *J. Mater. Civ. Eng.* 2011;23(February):100–109.

10. Van Jaarsveld JG., van Deventer JS., Lukey G. The effect of composition and temperature on the properties of fly ash- and kaolinite-based geopolymers. *Chem. Eng. J.* 2002;89(1-3):63–73.

11. Xu H, Van Deventer JSJ. Microstructural characterisation of geopolymers synthesised from kaolinite/stilbite mixtures using XRD, MAS-NMR, SEM/EDX, TEM/EDX, and HREM. *Cem. Concr. Res.* 2002;32(11):1705–1716.

12. Xu H, van Deventer JSJ. The effect of alkali metals on the formation of geopolymeric gels from alkali-feldspars. *Colloids Surfaces A Physicochem. Eng. Asp.* 2003;216(1-3):27–44.

13. Chakraverty A, Mishra P, Banerjee HD. Investigation of combustion of raw and acid-leached rice husk for production of pure amorphous white silica. *J. Mater. Sci.* 1988;23:21–24.

14. Granizo ML, Blanco MT. Alkaline Activation of Metakaolin An Isothermal Conduction Calorimetry Study.pdf. 1998:957–965.

15. Monzó M, Vicent M, Palomo A, Barba A. Activación alcalina de metacaolín. Efecto de la adición de silicato soluble y de la temperatura de curado. *Cerámica y Vidr.* 2008;47(1):35–43.

16. Delair S, Prud'homme É, Peyratout C, et al. Durability of inorganic foam in solution: The role of alkali elements in the geopolymer network. *Corros. Sci.* 2012;59:213–221.

17. Phair JW, Van Deventer JSJ, Smith JD. Mechanism of Polysialation in the Incorporation of Zirconia into Fly Ash-Based Geopolymers. *Ind. Eng. Chem. Res.* 2000;39(8):2925–2934.

18. Lee WKW, van Deventer JSJ. Use of Infrared Spectroscopy to Study Geopolymerization of Heterogeneous Amorphous Aluminosilicates. *Langmuir*. 2003;19(21):8726–8734.

Chapter 3

Metakaolin-based geopolymers for targeted adsorbents to heavy metal ion separation.

3.1. Introduction

The presence of the toxic metals generated by mineral processing in industries causes a major hazard to the water environment[1]. Thus, serious regulations are required to establish in many countries to remove effectively the toxic metal ions from the waste waters prior to discharge into natural environment. Also, metal ions are non-biodegradable materials and excessive levels can be damaging to human organism. Since, contamination of metal ions has a serious influence in the public health. Therefore, the elimination of metal ions from industrial waste to water is necessary to solve the environment of water cleaning. During the last few years, the common methods available to remove metal ions from waste water are coagulation, chemical precipitation, ion-exchange, and reverse osmosis[2]. In addition, the adsorption technique present excellent qualities for treating industrial waste waters containing metal ions, when solid adsorbents are employed for recovery of metal ions as lead, copper, cadmium, nickel and zinc[3]. Therefore, in the approach to replace the conventional adsorbents, geopolymers are a new strategy for decontamination of metal ions from waste water, which are composed of silica and alumina similar to zeolite material.[4–8] For this reason, the geopolymers has begun to develop as

adsorbent materials in the process of removal metal ions from the waste water as an alternative to the industrial sector[8]. It is known that geopolymers are alkali activated aluminosilicates, consisting of a solid reactive component that contains SiO_2 and Al_2O_3, for example, fly ashes, active clays, pozzolanas and slags[9,10]. The alkaline activation solution for geopolymerization process contains alkali hydroxides, silicates, aluminates, carbonates, and sulphates or combinations thereof[9]. Several researches used MK as ideal raw material for manufacture geopolymers[11,12] because of its high reactivity and purity compared to other clays[13,14]. Here, zeolite which present crystalline nature is well known as representative solid adsorbent for metal ions. Noticing is very meaningful that geopolymers have an amorphous three-dimensional structure constituted by SiO_4 and AlO_4 tetrahedra and can be prepared at lower temperature than zeolites. These geopolymers would expect to have the unique properties as well as zeolite adsorbents. Furthermore, the geopolymers became an important subject in following properties: compressive strength of the matrix and resistance to acid attack, freezing and heat thaw cycles. Such characteristic makes them interesting products for adsorbents as used with concrete replacements in various environments. If geopolymers can actually remove metal ions from waste water via adsorption, the regenerated matrix could become new approach for several industries. Consequently, this affects both the environment and societies positively[15–17]. However, existing literature on the adsorption of heavy metals using geopolymers is very little. Among them, Xu et al. reported the conversion of fly ash to geopolymer was investigated under different conditions for adsorbents. It was paid great attention as a potential material that geopolymers showed removal of Cd, Ni, Pb(II), Cu(II),

phosphate, NO_x, boron, fluoride, radionuclide of ^{137}Cs and ^{90}Sr, and dyes[18,19]. However, the details about geopolymer adsorbents still are not well known at this time. In the present work, the main aim is to synthesis of amorphous geopolymers from MK and silica fume in order to use the materials as adsorbents for decontamination of heavy metal ions including Cs^+ and Pb^{2+}. The preparation and metal adsorption of the geopolymers were focused in different Si and Al amount in the resultant matrix. The adsorption behavior was examined in a mixture of aqueous solution in detail for targeted separation of Cs^+ and Pb^{2+} ions.

3.2. Experimental.

3.2.1. Materials and geopolymer synthesis.

The MK was produced by the calcination of the kaolinite [$Al_2Si_2O_5(OH)_4$] at 700 °C for 5 h[20,21] and was used as Al_2O_3 source for the synthesis of geopolymers. Also, silica fume AEROSIL 380 purchased from EVONIK industries was used. The role of adding silica fume was to support the sufficient amount of SiO_2 on the resulting geopolymers. For the alkaline activator, aqueous sodium hydroxide (NaOH) was mixed with the silica fume (SiO_2) using a ratio of Na/Si = 0.6. Figure 3.1 shows the illustration of synthesis protocol of MK based geopolymer. MK was mixed in aqueous NaOH 8 M using a ball mill for 5 h with ratio of H_2O/Na = 10. Here, the molar ratio between SiO_2 and Al_2O_3 was changed at Si/Al = 1, 2, 3, 4, and 5. Then, the mixed pastes were casting into 20 mm latex cube molds and vibrated for 5 min to release the airs bubbles. The geopolymer pastes were cured at 80 °C for 12 h to start condensation reaction. Upon removal from the molds, the resultant geopolymers were placed in an

oven at 200 °C for 12 h in order to complete the polycondensation. Principal composition of raw materials for geopolymers is presented in Table 3.1.

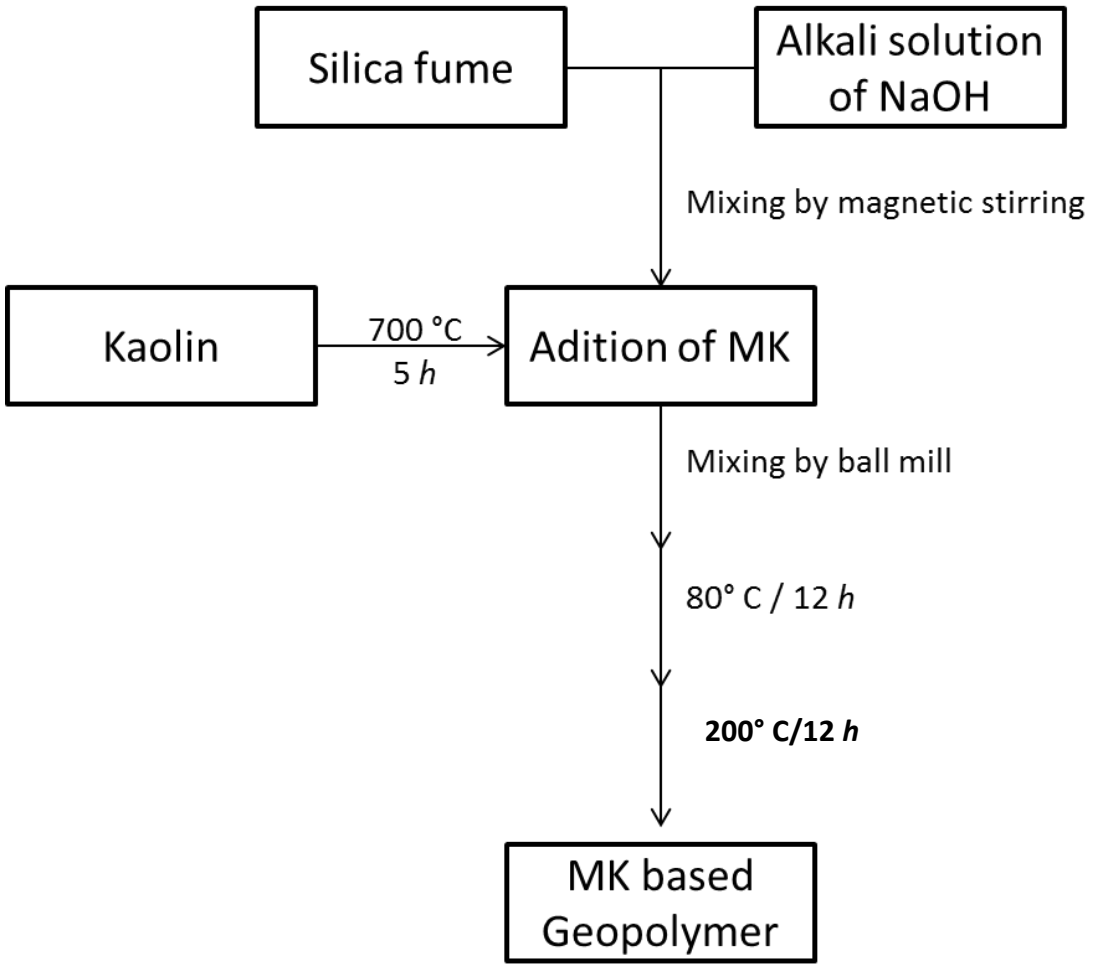

Fig. 3.1. Synthesis protocol of MK based geopolymer.

Table 3.1. Chemical composition of the MK-based geopolymer adsorbent.

Component	SiO_2 [%]	Al_2O_3 [%]	Fe_2O_3 [%]	CaO [%]	MgO [%]	K_2O [%]	Na_2O [%]	TiO_2 [%]
Silica Fume	99.9	0.01	---	---	---	---	---	0.01
MK	52	42.8	0.6	0.2	---	0.5	0.6	1.2
GP-1-0.6-10	48.4	41.2	0.56	0.19	---	0.46	1.92	1.12
GP-2-0.6-10	60.2	26.4	0.69	0.23	---	0.58	7.53	1.39
GP-3-0.6-10	65.3	18.7	0.75	0.25	---	0.63	6.29	1.51
GP-4-0.6-10	72.3	16.3	0.83	0.29	---	0.69	6.2	1.67
GP-5-0.6-10	73.7	12.7	0.85	0.28	---	0.71	5.96	1.7

3.2.2. Characterization of resultant MK-based geopolymers.

The obtained geopolymers were washed several times by deionized water in order to remove the excess of sodium hydroxide. After drying, the samples were crushed and sieved using a 120 mesh to control a particle size range. Before the adsorption tests of metal ions, the powder samples were characterized by FT-IR spectroscopy for determination of molecular vibration of the geopolymers, X-ray diffractometer (XRD) for crystal structure determination, X-ray fluorescence (XRF) in order to know chemical composition of principal components and Scanning electron microscopy (SEM) was used for evaluation of geopolymers morphology. The Brunauer–Emmer–Teller (BET) surface area was measured by a N_2 adsorption–

desorption after drying at 200 °C and the zeta potential was measured on a potentiometer (ELSZ1NGK Photal Otsuka Electronics instrument) in the absence and presence of 5 wt% and 10 wt% of NaCl at pH 5.

3.2.3. Adsorption tests of geopolymers for heavy metal ions.

The adsorption experiments of the geopolymers were performed by the batch system at 25 °C and pH 5. Multicomponent aqueous solutions containing Cs^{+}, Pb^{2+}, Cu^{2+}, Cd^{2+}, Ni^{2+} and Zn^{2+} were chiefly prepared from analytical grade standard solutions (Nakarai Teque, Japan) in the range of 50 to 500 mg/L. The initial pH of the heavy metal solution was controlled to pH 5 with adjusting amounts of HCl 0.1M and NaOH 0.1M for each adsorption test. Then 0.05 mg of geopolymer powder was added in 40 ml of the multicomponent aqueous solution of metal ions. After adsorption batch, the supernatant liquid was separated by centrifugation at 100 rpm. The changes in the metal ion contents in the supernatant were analyzed by atomic absorption spectroscopy (AA-6300 SHIMADZU). The changes in metal ion concentration of the solution were represented as the removal of metal ion by geopolymer adsorption, according to following equation.

$$q_e = \frac{(C_0 - C_e)V}{W} \quad (10)$$

where C_0 and C_e are the initial and equilibrium concentrations (ppm), respectively, of the metal ion in the solution, V is the volume (L), and W is the weight (mg) of the adsorbent.

3.3. Results and discussions.

3.3.1. Properties of geopolymer adsorbents.

Table 3.2 shows the surface area (BET), zeta potential at pH 5 and bulk density of the MK based geopolymers. By using the chemical composition by XRF data we estimated Si/Al ratio in the geopolymers after the polycondensation reaction and it was observed that the values of the ratio were close to the calculated in the beginning. This meant that the polycondensation of MK and silica fume was performed to be geopolymer framework under the described conditions.

Table 3.2. Composition and condition of geopolymer synthesis

Sample	Si/Al	Na/Si	H_2O/Na	Si/Al by XRF	BET [m^2/g]	ζ-Potential at pH = 5 [mV]	Bulk density [g/cm^3]
GP-1-0.6-10	1	0.6	10	0.99	27.5	-20.0	0.8
GP-2-0.6-10	2	0.6	10	1.91	3.3	-29.0	0.68
GP-3-0.6-10	3	0.6	10	2.84	2.3	-29.0	1.09
GP-4-0.6-10	4	0.6	10	3.72	1.9	-29.0	1.41
GP-5-0.6-10	5	0.6	10	4.86	2.1	-28.3	1.23

*The curing temperature for the condensation was carried out at 80° C for 12 hours and then cured again at 200 °C for 6 hours.

SEM pictures are shown in Figure 3.2, the resultant geopolymers with a ratio Si/Al > 4 were condensed like a dense matrix as seen in Fig. 3.2d) and Fig. 3.2e). The morphology suggested that the grain size of the geopolymers was decreased with increasing the amount of silica in the framework. Correspondingly, the surface area

BET was higher in the GP-1-0.6-10 than those of others due to the high Al content in the geopolymer. Also, an increase of the bulk density was observed, leading the decreasing of the porosity in the samples. FTIR spectra are shown in Figure 3.3. The spectral data of MK and silica fume used as raw materials were included. The spectral differences in the FTIR results were found in the low-wavenumber region between 800 to 400 cm^{-1} and the middle-wavenumber region between 1250 to 800 cm^{-1}. In the low-wavenumber region, the spectrum of silica fume had characteristic the bands at 469 cm^{-1} assigned to Si-O tetrahedral bending vibration and the MK band at 461 cm^{-1} and 812 cm^{-1} assigned to tetrahedral bending mode of T-O (T = Si or Al) and bending mode of Si-O-Al[22,23], respectively. After geopolymerization, both intensities of these two bands decreased and the new band appeared at about 710 cm^{-1}. The spectral data indicated that the formation of tetrahedral Al [Al-O_4] was found in the resultant geopolymers[23]. The small band appearing around 1400 cm^{-1} was related to the asymmetric stretching of the O-C-O bonds of CO_3^{2-} due to atmospheric carbonation on the surface of powdered products[24]. The absorption bands at 1650 cm^{-1} was for H-OH vibration, corresponding to the presence of water in the geopolymer[22]. Moreover, the small band centered about 600 cm^{-1} was caused by T-O-Si symmetric stretching vibrations. In the mid-wavenumber region, a shift in the broad band position for Si-O-Si of silica fume at 1099 cm^{-1} and Si-O-T from MK at 1084 cm^{-1} was seen toward 1000 cm^{-1}. Both assigned asymmetric stretching peaks were seen in the geopolymer as assigned to Si-O-Al of geopolymer vibration at 1000 cm^{-1}.[25] This band shift suggested strongly formation of geopolymers[26,27]. Especially, at higher Si/Al ratio, the Si-O-Si band at 1099 cm^{-1} was observed in the broad band as shoulder.

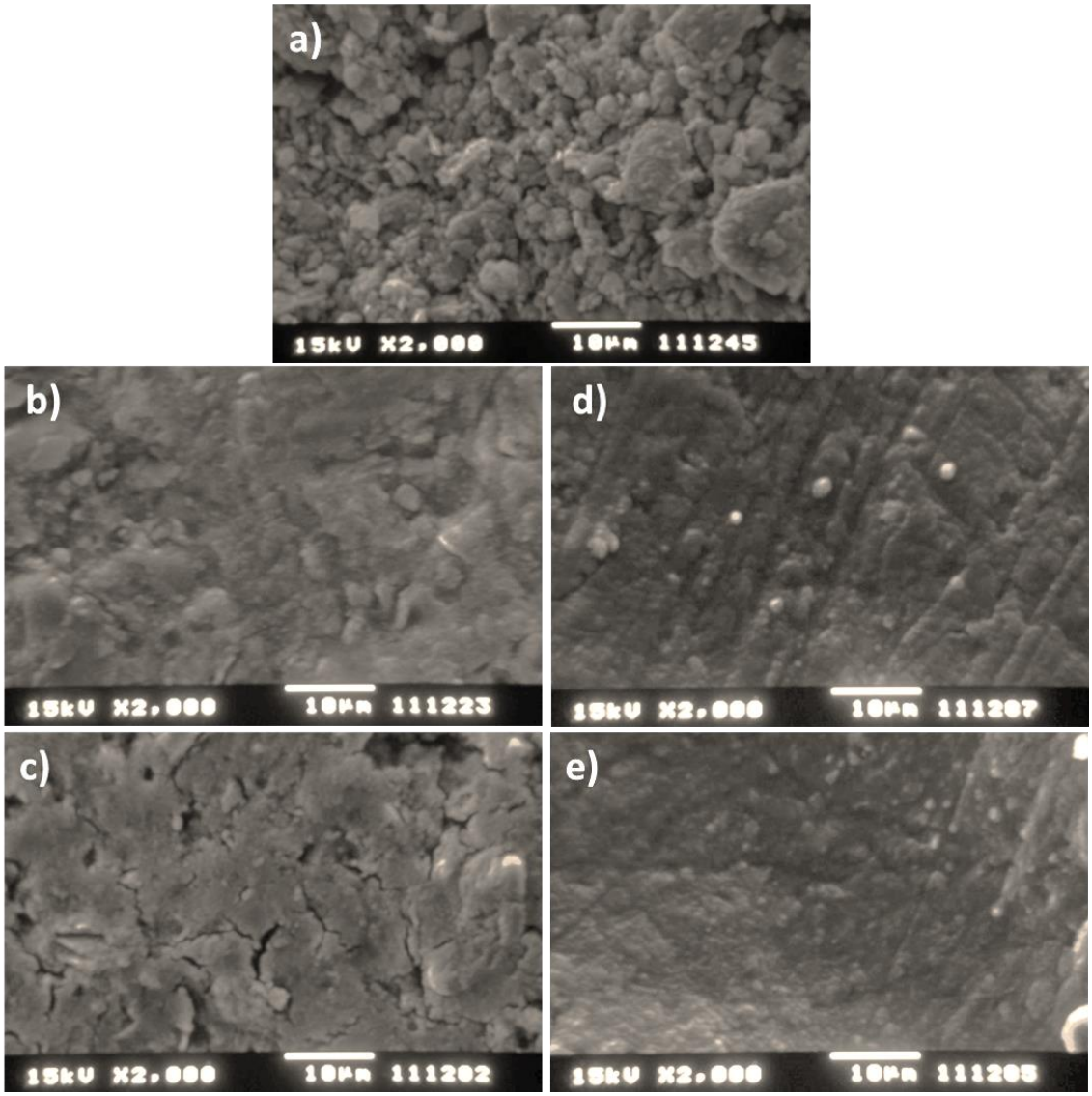

Fig. 3.2. SEM micrographs of the MK based geopolymers: a) GP-1-0.6-10, b) GP-2-0.6-10, c) GP-3-0.6-10, d) GP-4-0.6-10 and e) GP-5-0.6-10.

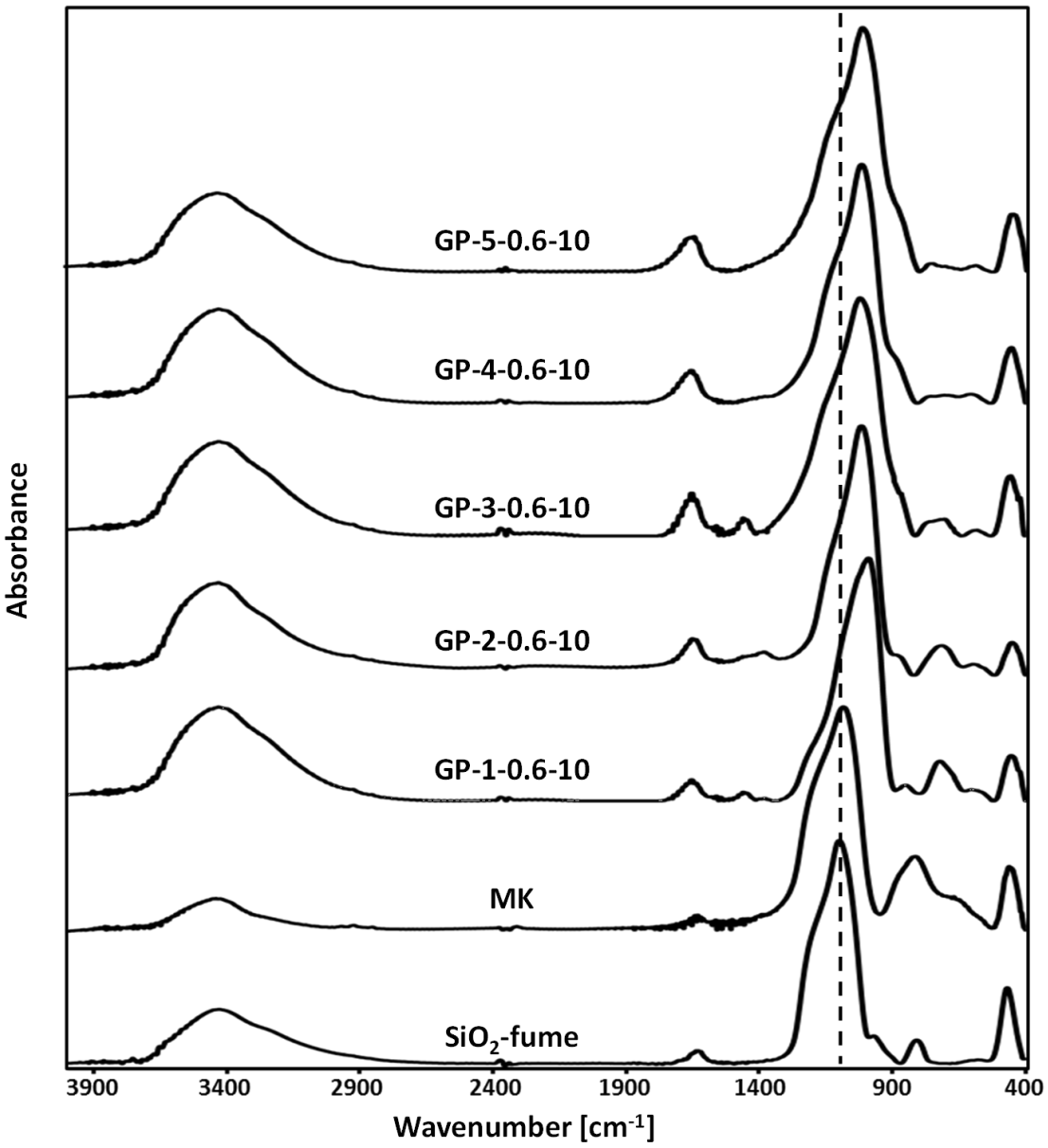

Fig. 3.3. FTIR spectra of raw material and synthesized MK based geopolymers.

Furthermore, the XRD pattern in Figure 3.4 supported the amorphous features of the geopolymers. As seen, the silica fume and MK used had broad peak centered at 22° in the XRD patterns. The presence of the sharp peak at 26° implied that the MK contained crystalline SiO_2 and mica components. After the alkali activation of the starting materials, the scattering diffraction of the broad peak was shifted from ~22° to ~28° in 2θ. This was evidence of the change in the local bonding environment due to the arrangement of the structure during the polycondensation process.

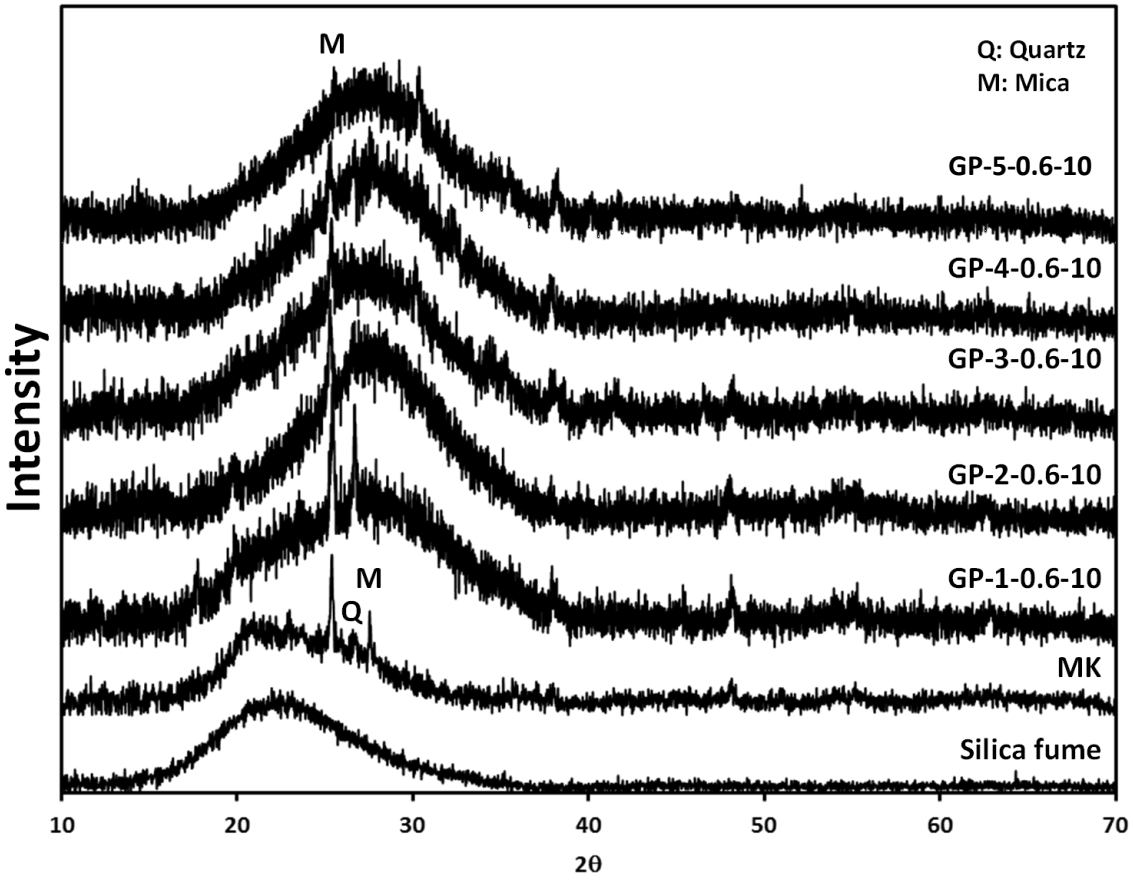

Fig. 3.4. XRD results of raw material and MK based geopolymers.

Table 3.2. contains the zeta potential obtained from the geopolymers at pH of 5. The values of zeta potential are shown in Figure 3.5. It was possible to observe that the zeta potential decreased from -20 mV to -29 mV when the Si/Al ratio was increased from 1 to 5, respectively, at pH 5. This meant that the increment in the silica content in the framework caused negatively changed groups of O-Si-O^- in the geopolymer[28] for the corresponding surface charges expressed. As shown in Figure 5, the values of zeta potential increased, when NaCl concentration increased at 5 and 10 wt%.The zeta potential increased with the increment of SiO_2 and a constant value was obtained after the ratio of Si/Al = 2, for the three NaCl concentrations. In other hand, it was observed the zeta potential decrease with the increment of concentration of NaCl of 5 % and 10 % due to the competitive adsorption of H^+ with Cl^- for the binding sites of geopolymers at pH 5. For example at Si/Al = 2, each value of zeta potential was changed from -29 mV, -22 mV and -15 mV with a [NaCl] = 0, 5 and 10 wt % concentration, respectively. This behavior indicated that the negatively charge was electro-statically shielded by the added salt.

3.3.2. Adsorption studies of MK-based.

The amount of silica fume in the MK based geopolymers adsorbents have a strong influence on the ad-sorption process. Figure 3.6 shows the analysis of Langmuir isotherms for single component of metal ion [Fig. 3.6a)] and multicomponent solution [Fig. 2.6b)] of metal ions of Pb^{2+}, Cu^{2+}, Cd^{2+}, Ni^{2+}, Zn^{2+} and Cs^+ adsorbed by geopolymers. For Fig. 3.6a) was observed that the adsorption by GP-2-0.6-10 for Pb^{2+}, Cu^{2+} and Cs^+ predominated to comparison of Cd^{2+}, Ni^{2+} and Zn^{2+}

which were less than the former ion group. At pH 5, Pb^{2+} could be present as $Pb(OH)^{+}$, $Pb_2(OH)^{3+}$, $Pb_3(OH)_4^{2+}$ and $Pb_4(OH)_4^{4+}$ but just in a small amounts[29]. However, the experiments of adsorption for Pb^{2+} could not be performed beyond pH 6.0 due to the low solubility of Pb^{2+} hydroxide in water,[30] because the lead component is formed as white precipitation at that pH. Therefore, the adsorption test was carried out at pH 5.

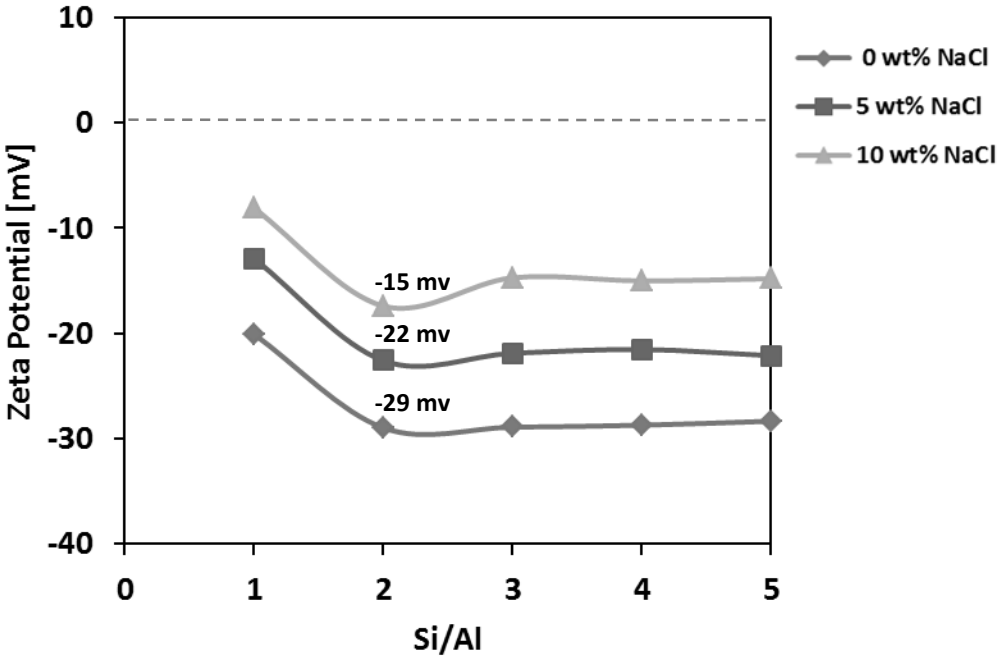

Fig. 3.5. Zeta potential in function of the ratio of Si/Al of MK based geopolymer with 0 wt% NaCl, 5 wt% NaCl and 10 wt % NaCl at pH 5

In contrast, the multicomponent system Fig. 3.6b) showed that the removal of Pb^{2+} and Cs^{+} increased considerately, especially for Cs^{+} ion. This comparison between Fig. 3.6a) and Fig. 3.6b) meant that the geopolymer had selective binding for Cs^{+}. As a result, the adsorption selectivity of GP-2-0.6-10 for a mixture of metal ions was in the

following order $Cs^{+}>Pb^{2+}>Cu^{2+}>Zn^{2+}>Ni^{2+}>Cd^{2+}$. Figure 3.7 shows adsorption behavior of Pb^{2+} for several geopolymers at different Si/Al ratio. It was noted that the GP-2-0.6-10 presented better adsorption for Pb^{2+}, in comparison with the GP-1-0.6-10 which containing higher Al amount in the framework, so that the adsorption for Pb^{2+} ions decreases. It is very interesting to study salt effect of adsorption behavior of the geopolymers. As shown in the results of zeta potential, negative value supported the presence of negatively electrostatic force on the geopolymers.

In Table 3.3 for GP-2-0.6-10, the effect of the addition of NaCl was tested with a concentration of 5 and 10 wt% on the mixture solution of metal ions. It is worth noting that the salt effect does not affect considerably in the adsorption of metal ions. For example, Cs^{+} was adsorbed on the geopolymer with q_m = 43, 42 and 43 mg/g for [NaCl] = 0, 5 and 10 wt%, respectivily. Similarly, insignificant changes were observed for the maximum adsorption by GP-2-0.6-10 of Pb^{2+} and the other metal ions with the increment of NaCl concentration as shows in Figure 3.8. As seen, the metal ions adsorption by geopolymer at pH 5 was indicated that sodium concentration had no effect on the adsorption of the heavy metal ions. This meant that the heavy metal ions captured by geopolymer might be due to the less effect of electrostatic mechanism. Langmuir equation with Sacatchard analisys was used for geopolymer adsorbents in modeling of the isotherm data for the multi-component solution containing Cs^{+}, Pb^{2+}, Cu^{2+}, $Cd2^{+}$, Ni^{2+} and Zn^{2+}.The experimental isotherms are useful for describing adsorption capacity to facilitate evaluation of the feasibility of this process.

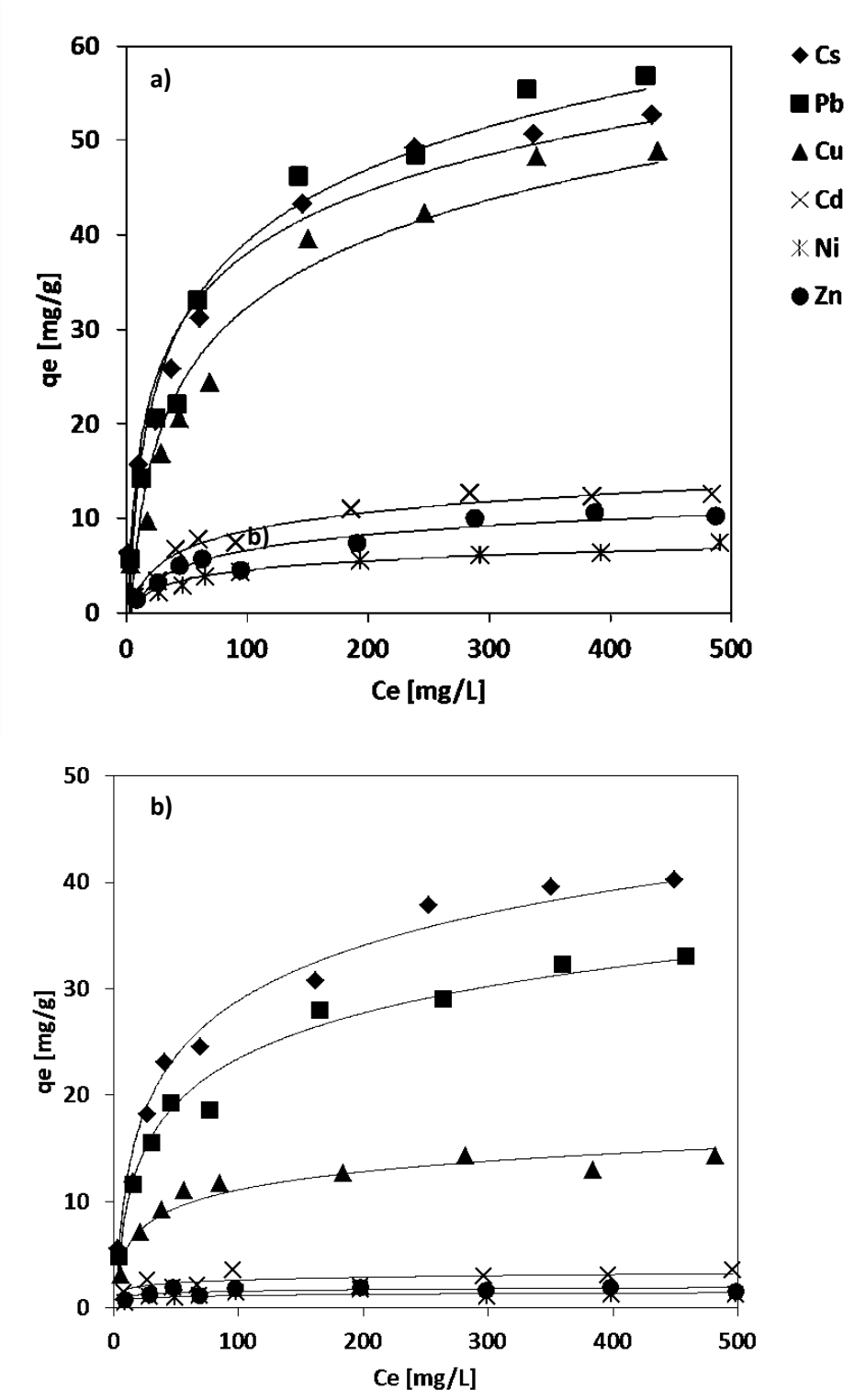

Fig. 3.6. Langmuir isotherms for the adsorption of a) individual metal ions solution and b) mixture of multicomponent of metal ions by GP-2-0.6-10.

The isotherm measures the relation between the equilibrium concentration of the adsorbate in the solid phase q_e [mg/g] and the equilibrium concentration in the aqueous phase C_e (mg/L). As known, various mathematical transformations of the classical Langmuir equation, $q_e = (q_m K_b C_e)/(1+K_b C_e)$, are presented and then, the analysis having transformations of C_e/q_e versus q_e, providing various useful graphical demonstration manners[31]. The Scatchard transformation can give more compact information about affinity phenomena of sorbent toward analyte. In the present study, the experimental data was applied to the Scatchard transformation was represented by the following equation:[32]

$$\frac{q_e}{C_e} = q_m K_b - q_e K_b \quad (11)$$

where q_m is theoretical maximum sorption capacity of sorbent for target solute to form a complete monolayer, and K_b is the constant related to affinity between sorbent and sorbate.

Table 3.3. NaCl addition to multi-component solution for the adsorption capacity of heavy metal by GP-2-0.6-10.

Metal Ion	0 wt% NaCl q_m [mg/g]	5 wt% NaCl q_m [mg/g]	10 wt% NaCl q_m [mg/g]
Cs^+	43	42	43
Pb^{2+}	35	34	35
Cu^{2+}	15	13	15
Cd^{2+}	3	3	3
Ni^{2+}	1	1	1
Zn^{2+}	2	2	2

The parameters calculated from the Scatchard plots are collectively listed in Table 3.4. As seen, Langmuir isotherm model was useful for characterization of specific bindings, because it mainly deal with sorption on specific binding sites. The Scatchard plot analysis for GP-2-0.6-10 is shown in Figure 3.9. The Scatchard plot is widely used technique in evaluating the affinities of binding sites taking role in a particular adsorption process from the slop and the extrapolation of the plot at $q_m = 0$. As can be seen, the deviation tendency in the plot from the linearity portion resulted in two independent sets in the data.

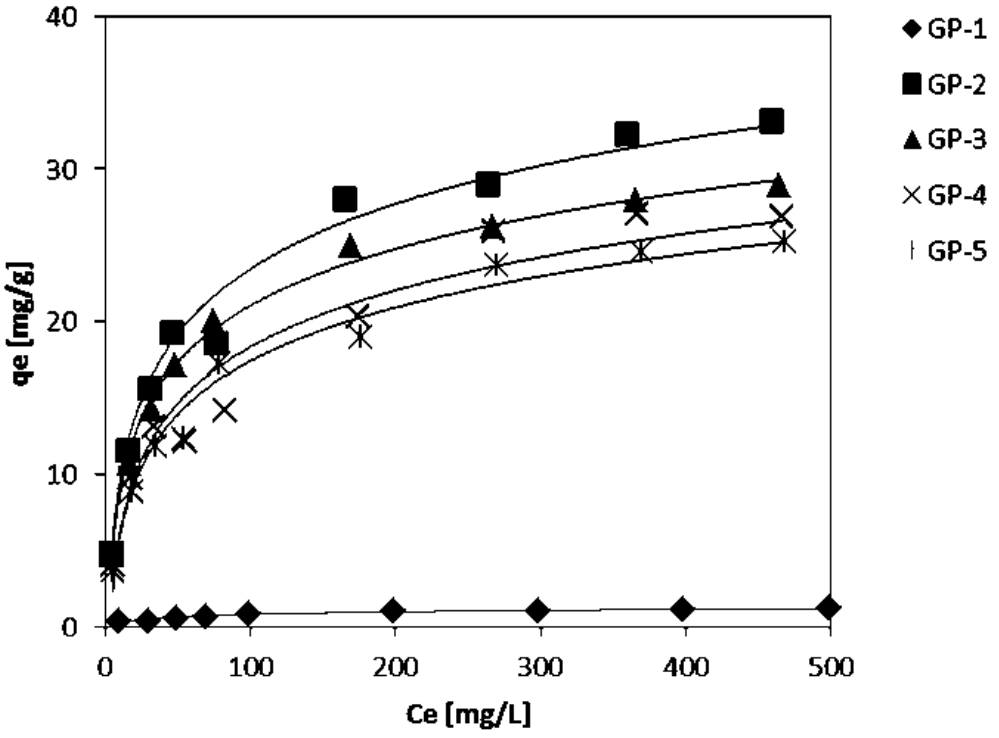

Fig. 3.7. Langmuir isotherms for the adsorption of Pb^{2+} by MK based adsorbents at pH 5

Table 3.4. Isotherm parameters of Scatchard plot.

Metal	q_m[µmol/g]		Kb[L/mol]	
Ion	H	L	H	L
Cs^+	193	435	20 000	2810.5
Pb^{2+}	139	306	18 000	3745.4
Cu^{2+}	197	932	12 000	743.4
Cd^{2+}	---	---	---	---
Ni^{2+}	---	---	---	---
Zn^{2+}	---	---	---	---

The *H* and *L* symbols represent particular parameters for high- and low-affinity bindings, respectively.

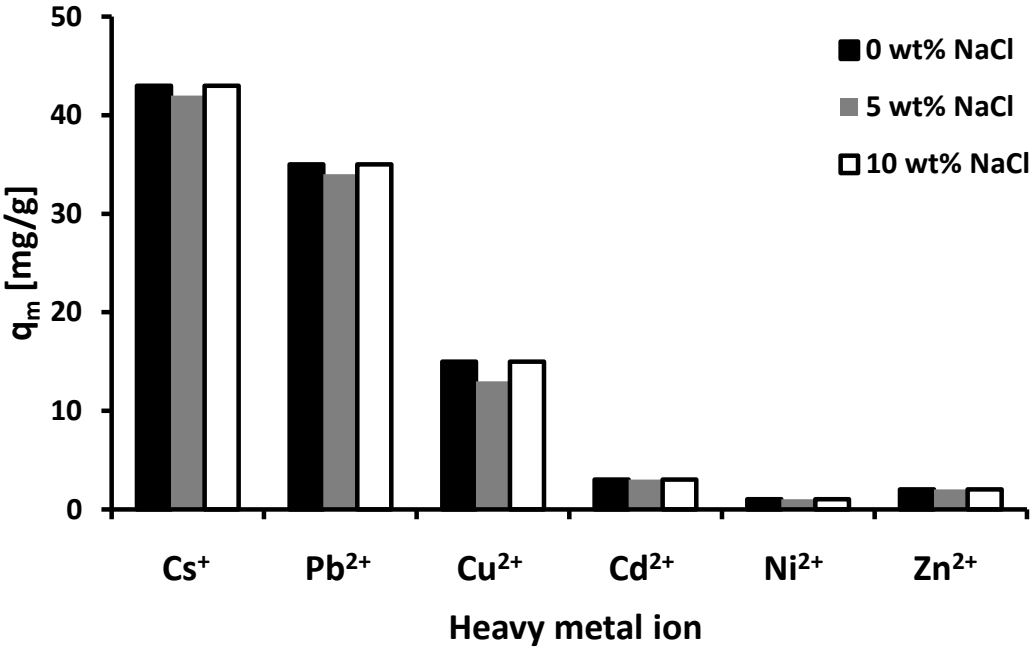

Fig. 3.8. Maximum adsorption capacity (q_m) of heavy metal ions by GP-2-0.6-10 with different concentration of NaCl. 0 wt% NaCl, 5 wt% NaCl and 10 wt % NaCl at pH 5.

This phenomenon indicated presence of at least two types of binding sites having different affinities toward the metal ions in the geopolymer system. So, the geopolymer adsorbent has high-affinity and low-affinity sites for Cs^{+} and Pb^{2+} ions. Hence, the observed linear data were believed to be separately related to different specific bindings. The separately calculated isotherm parameters are tabulated in Table 3.4. Here, two different specific binding types of metal ions on the geopolymer were found to be observable at pH 5 as designated with *H* and *L*, representing high and low affinity. It can be suggested that the specific binding sites of Cs^{+} and Pb^{2+} were contained mainly in the geopolymer. This information can be useful in design of novel separation techniques based on adsorption process for selective removal metal ions from waste water. Therefore, furthermore, research would be on the progress on the clear explanation of the adsorption behavior. Additionally, it was interesting to note that in Figure 3.6 the high binding Pb^{2+} ion was observed in the single ion system [Fig. 3.6a)], but the order in Pb^{2+} and Cs^{+} was changed for the multicomponent system [Fig. 3.6b)]. This meant that predominant adsorption to Cs^{+} was occurred in the geopolymer adsorbent, when Pb^{2+} and Cs^{+} were competed in the adsorption. As mentioned, the Scatchard analysis of q_m and K_b were supported the strong Cs^{+} binding to the geopolymers.

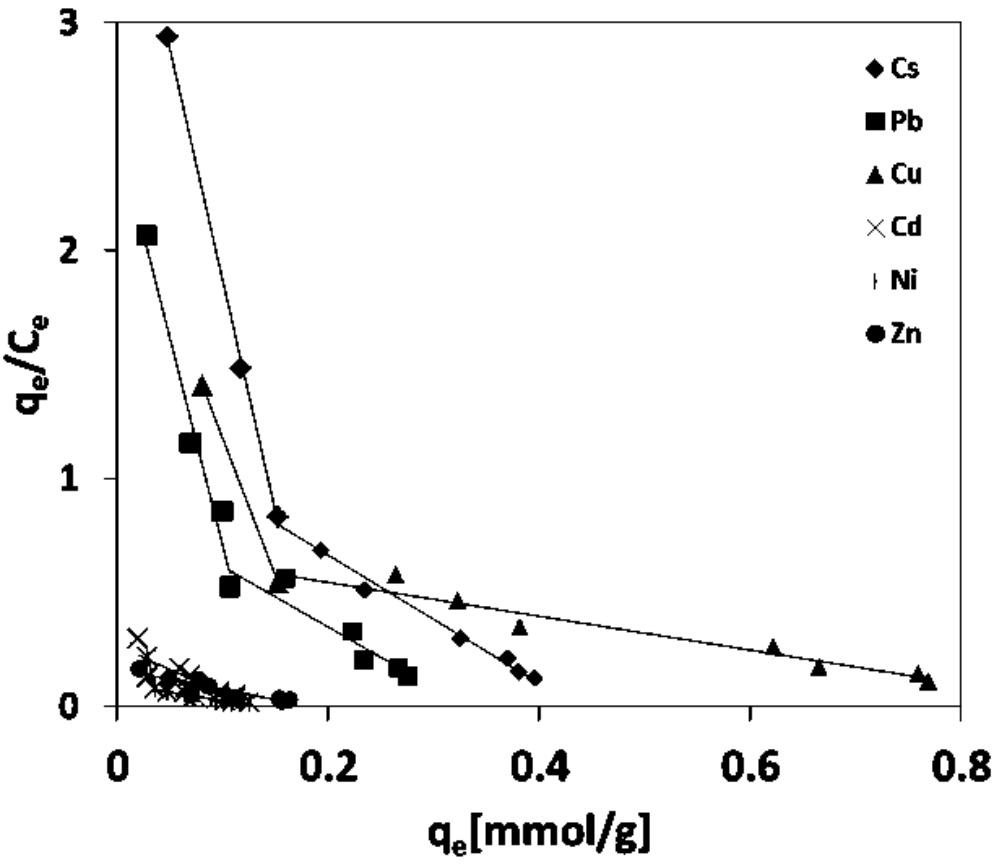

Fig. 3.9. The Scatchard plot analysis for GP-2-0.6-10 at pH 5

3.4. Conclusion

On the ability of MK-based geopolymers, the removal of Cs^{+} and Pb^{2+} with heavy ion mixture of Cu^{2+}, Cd^{2+}, Ni^{2+} and Zn^{2+} was conducted from aqueous solution of mixed heavy metals. The adsorbent behavior was examined as function of the Si/Al ratio in the geopolymer matrix and optimized at Si/Al=2. The geopolymer worked well for the separation of Pb^{2+} and Cs^{+} on the mixture solution of metal ions. The value of the adsorption capacity increased in the following order: $Cs^{+} > Pb^{2+} > Cu^{2+} > Cd^{2+} > Ni^{2+} > Zn^{2+}$ for the mixture of the multicomponent system, while the individual

experiment showed higher adsorption in Pb^{2+} relative to Cs^{+}. Langmuir adsorption model was used for analyzing the efficiency of adsorption of the metal ions onto geopolymers. This suggested that the geopolymer adsorbents have a high selectivity for Cs^{+} ion. Salt effect on the adsorption behavior indicated that the selectivity was due to the electrostatic force of charged sites of the geopolymers. For evaluating the type of interactions between metal ions and MK-based geopolymer, further research would be in progress in near future.

3.5. Reference.

1. Matis KA, Zouboulis AI, Lazaridis NK. Removal and Recovery of Metals from Dilute Solutions. *Miner. Process. Environ.* 1998;43:165–196.

2. Hui KS, Chao CYH, Kot SC. Removal of mixed heavy metal ions in wastewater by zeolite 4A and residual products from recycled coal fly ash. *J. Hazard. Mater.* 2005;127(1-3):89–101.

3. López FA, Martín MI, Pérez C, López-Delgado A, Alguacil FJ. Adsorción de metales pesados sobre cascarilla de laminación. *Rev. Met. Madrid*. 2003;39:215–223.

4. Buchwald a., Zellmann H-D, Kaps C. Condensation of aluminosilicate gels—model system for geopolymer binders. *J. Non. Cryst. Solids*. 2011;357(5):1376–1382.

5. Komnitsas K, Zaharaki D. Geopolymerisation: A review and prospects for the minerals industry. *Miner. Eng.* 2007;20(14):1261–1277.

6. Xu H, Van Deventer JSJ. Microstructural characterisation of geopolymers synthesised from kaolinite/stilbite mixtures using XRD, MAS-NMR, SEM/EDX, TEM/EDX, and HREM. *Cem. Concr. Res.* 2002;32(11):1705–1716.

7. Barbosa VFF, MacKenzie KJD. Synthesis and thermal behaviour of potassium sialate geopolymers. *Mater. Lett.* 2003;57(9-10):1477–1482.

8. Xu H, Van Deventer JSJ. The geopolymerisation of alumino-silicate minerals. *Int. J. Miner. Process.* 2000;59(3):247–266.

9. Prud'homme E, Michaud P, Joussein E, Peyratout C, Smith a., Rossignol S. In situ inorganic foams prepared from various clays at low temperature. *Appl. Clay Sci.* 2011;51(1-2):15–22.

10. Zhang YJ, Li S, Wang YC, Xu DL. Microstructural and strength evolutions of geopolymer composite reinforced by resin exposed to elevated temperature. *J. Non. Cryst. Solids*. 2012;358(3):620–624.

11. Duxson P, Fernández-Jiménez a., Provis JL, Lukey GC, Palomo a., Deventer JSJ. Geopolymer technology: the current state of the art. *J. Mater. Sci.* 2006;42(9):2917–2933.

12. Goretta KC, Gutierrez-Mora F, Singh D, Routbort JL, Lukey GC, Deventer JSJ. Erosion of geopolymers made from industrial waste. *J. Mater. Sci.* 2007;42(9):3066–3072.

13. Kong DLY, Sanjayan JG, Sagoe-Crentsil K. Comparative performance of geopolymers made with metakaolin and fly ash after exposure to elevated temperatures. *Cem. Concr. Res.* 2007;37(12):1583–1589.

14. Cheng TW, Lee ML, Ko MS, Ueng TH, Yang SF. The heavy metal adsorption characteristics on metakaolin-based geopolymer. *Appl. Clay Sci.* 2012;56:90–96.

15. Li L, Wang S, Zhu Z. Geopolymeric adsorbents from fly ash for dye removal from aqueous solution. *J. Colloid Interface Sci.* 2006;300(1):52–9.

16. Wang S, Peng Y. Natural zeolites as effective adsorbents in water and wastewater treatment. *Chem. Eng. J.* 2010;156(1):11–24.

17. Zhang J, Provis JL, Feng D, van Deventer JSJ. Geopolymers for immobilization of Cr(6+), Cd(2+), and Pb(2+). *J. Hazard. Mater.* 2008;157(2-3):587–98.

18. Ahmaruzzaman M. A review on the utilization of fly ash. *Prog. Energy Combust. Sci.* 2010;36(3):327–363.

19. López FJ, Sugita S, Takaomi K. Cesium-adsorbent Geopolymer Foams Based on Silica from Rice Husk and Metakaolin. *Chem. Lett.* 2014;43(1):128–130.

20. Palomo a., Blanco-Varela MT, Granizo ML, Puertas F, Vazquez T, Grutzeck MW. Chemical stability of cementitious materials based on metakaolin. *Cem. Concr. Res.* 1999;29(7):997–1004.

21. Granizo ML, Blanco-Varela MT, Palomo A. Influence of the starting kaolin on alkali-activated materials based on metakaolin . Study of the reaction parameters by isothermal conduction calorimetry. *J. Mater. Sci.* 2000;32:6309–6315.

22. Parker RW, Frost RL. The application of drift spectroscopy to the multicomponent analysis of organicchemicals adsorbed on montmorillonite. 1996;44(1).

23. Rios C, Williams C, Fullen M. Nucleation and growth history of zeolite LTA synthesized from kaolinite by two different methods. *Appl. Clay Sci.* 2009;42(3-4):446–454.

24. Giannopoulou I, Panias D. Hydrolytic stability of sodium silicate gels in the presence of aluminum. *J. Mater. Sci.* 2010;45(19):5370–5377.
.

25. Ortego JD, Barroeta Y, Cartledge FK, Akhter H, Rouge B. Leaching Effects on Silicate Polymerization. An FTIR and 29Si NMR Study of Lead and Zinc in Portland Cement. 1991;174(11):1171–1174.

26. Granizo ML, Blanco MT. Alkaline Activation of Metakaolin An Isothermal Conduction Calorimetry Study.pdf. 1998:957–965.

27. Zhang Y, Sun W, Li Z. Infrared spectroscopy study of structural nature of geopolymeric products. *J. Wuhan Univ. Technol. Sci. Ed.* 2008;23(4):522–527.

28. Aranberri I, Bismarck A. Caracterización superficial de minerales arcillosos presentes en los depósitos de crudo. *An. Quim.* 2007;103(2):23–27.

29. Sreejalekshmi KG, Krishnan KA, Anirudhan TS. Adsorption of Pb(II) and Pb(II)-citric acid on sawdust activated carbon: Kinetic and equilibrium isotherm studies. *J. Hazard. Mater.* 2009;161(2-3):1506–13.

30. Sen Gupta S, Bhattacharyya KG. Immobilization of Pb(II), Cd(II) and Ni(II) ions on kaolinite and montmorillonite surfaces from aqueous medium. *J. Environ. Manage.* 2008;87(1):46–58.

31. Gezici O, Kara H, Ayar A, Topkafa M. Sorption behavior of Cu(II) ions on insolubilized humic acid under acidic conditions: An application of Scatchard plot analysis in evaluating the pH dependence of specific and nonspecific bindings. *Sep. Purif. Technol.* 2007;55(1):132–139.

32. Bhattacharya AK, Venkobachar C. Removal of Cadmium (II) by Low Cost Adsorbents. *J. Environ. Eng.* 1984;110(1):110–122.

Chapter 4

Cesium-adsorbent Geopolymer Foams Based on Silica from Rice Husk and Metakaolin

4.1 Introduction.

As is well known, aluminosilicates inorganic adsorbents to cesium with zeolites, which are materials to clean-up radioactive cesium. In addition, aluminosilicate materials as geopolymers have received special attention because they possess adsorbent properties that can support the removal of metals from wastewater.[1,2] The removal of metals by a geopolymer is feasible due to its three-dimensional polymeric structure. This structure includes pores formed during the condensation of aluminosilicate minerals by alkali activation at a temperature below 200° C.[3–6] Moreover, geopolymers have several other advantages such as resistance to stress, heat, and chemical attack.[7,8] Moreover, effectively solidified geopolymers can actually remove heavy metal ions from wastewater via adsorption.[9] This proposed method becomes a new strategy for toxic waste treatment, affecting both the environment and the society positively. However, there are very few existing adsorbent geopolymers. Therefore, in the present study, new geopolymer foams elaborated with MK and silica obtained from RH and their applications for cesium adsorption are reported.

4.2 Experimental and results.

First, we prepared raw materials from dehydroxylated kaolinite to obtain MK[10] and silica from the combustion of RH from Japan.[11] It has been reported that MK acted as the aluminum source in geopolymers, since its high pozzolanic property was suitable for geopolymer condensation in a nonformed one.[12–15] RHA containing a high percentage of reactive silica was used as the pozzolan and was adjusted for the SiO_2 content of the geopolymer mixture[16,17] to produce inorganic foam. Therefore, in the present work, we synthesized three geopolymer foams with different molar ratios of SiO_2 and Al_2O_3 (Si/Al). The sodium ratio and water ratio were maintained constant for each geopolymer foam. Alkali activation was carried out by dissolving the silica from the RHA (specific surface area: 207.5 m^2/g) and NaOH pellets (97% purity) in distilled water. MK (specific surface area: 11.5 m^2/g) was added after the dissolution of silica. Additionally, the chemical composition of RHA and MK was examined by XRF analysis and confirmation without any toxic heavy metals was performed. The reactive mixtures of the alkali activated solution of MK and RHA were then added in a sealed polystyrene mold and placed in an oven at 100° C for 12 h to complete the polycondensation reaction. Subsequently, the samples were removed from the mold and kept at 150° C for 2 h. In the experiments, three geopolymer foams at different Si/Al ratios of 2.5, 5, and 10 were produced and designated as GP-2.5-0.6-10, GP-5-0.6-10, and GP-10-0.6-10. The obtained geopolymers foams were washed several times with deionized water in order to remove excess sodium hydroxide until the pH was around 7. As shown in Table 4.1, the values of Si/Al in the geopolymer were evaluated by XRF. The surface area was measured by the N_2 gas adsorption BET

method. Figure 4.1 shows images of the geopolymer foam synthesized by the polycondensation of RHA and MK. The cross-section shows the porous material with a sponge structure. It was observed that foam formation was caused by water vapor when the polycondensation reaction was complete at 150° C.[18–21]

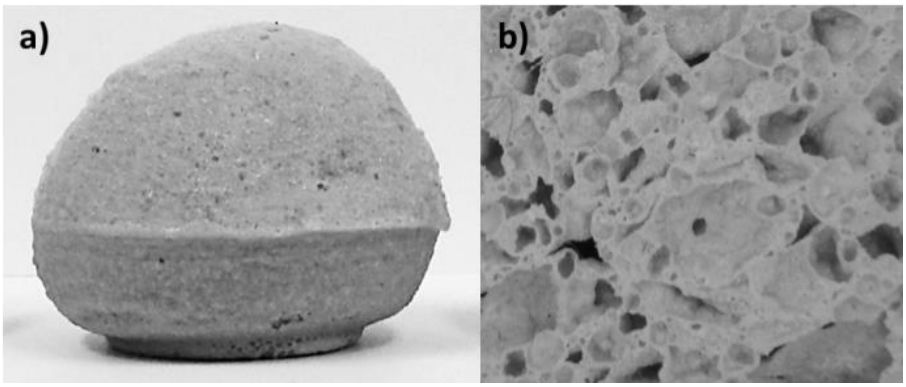

Fig. 4.1. a) Geopolymer foam synthesized and b) cross-section of geopolymer foam showing the porous body for GP-2.5-0.6-10.

Table 4.1. Surface area and bulk density of geopolymer foams.

Sample	(Si/Al) Feeding	(Si/Al) Measured by XRF	Surface area (m^2/g)	Bulk density (g/ml)
GP-2.5-0.6-10	2.5	2.7	0.42	0.94
GP-05-0.6-10	5.0	4.6	0.34	0.88
GP-10-0.6-10	10	9.1	0.94	0.80

The adsorption experiments were performed using the washed geopolymers as adsorbents for cesium. Cesium solution was prepared from analytical grade standard solutions for metal ion concentrations in the range of 50 to 500 mg/l, then 0.2 g of geopolymer were added to 40 ml of cesium ion solution, subsequently the pH was

adjusted and shaking in a bath for 6 h at 30° C. After the adsorption experiments were finished, the solution was separated via centrifugation and collected for testing by spectroscopy atomic absorption analysis. The changes in cesium concentration in the solution were represented as the removal of cesium metal by geopolymer adsorption. The obtained results from the residual solution analysis express the residual concentration of cesium ion. The amount of the adsorbed ion was calculated by subtracting residual concentration from initial concentration. The maximal amount of metal ion adsorption q_m and the Langmuir constant K_L were determined from the intercept and the slope of the plot.

Figure 4.2 shows the XRD data of raw materials and each foam obtained after geopolymerization reaction, showing their amorphous features. The transformation of raw materials during geopolymerization was shown in the diffraction pattern by shifting in the scattering diffraction peak of foams obtained from RHA and MK. The scattering diffraction peak shifted from ~20° to ~28° in 2θ after the polycondensation reaction. This shift demonstrates the formation of new amorphous phase described as geopolymeric material.

The SEM images (Figure 4.3) show the modifications by RHA in terms of the porosity size and distribution of the samples: GP-10-0.6-10 presents a pore network smaller than that observed in GP-2.5-0.6-10 and GP-5-0.6-10. The low silica content in the samples leads to a decrease in the viscosity of the activated alkali solution, which involves pore coalescence, resulting in large pores. The same effect was observed in the surface area, bulk density, and bulk molar ratio (Table 4.1). No significant change

was observed in the Si/Al ratio before and after the geopolymerization. This result was confirmed by XRF, as shown in Table 4.1. Moreover, the surface area decreased considerably in comparison with the raw material. This implies that geopolymers are porous and play an important role in the adsorption action of cesium.

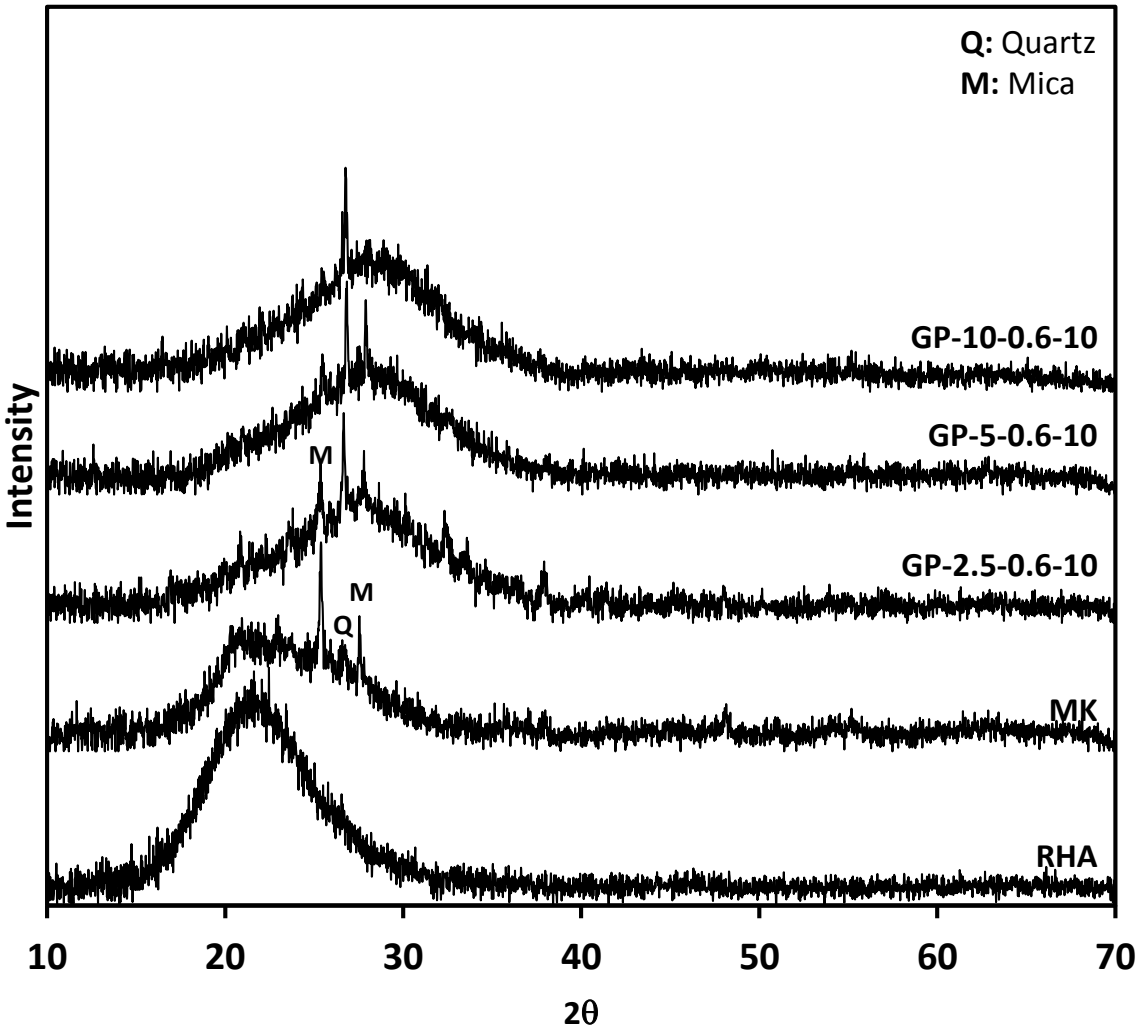

Fig. 4.2. XRD patterns of raw material and geopolymer foams.

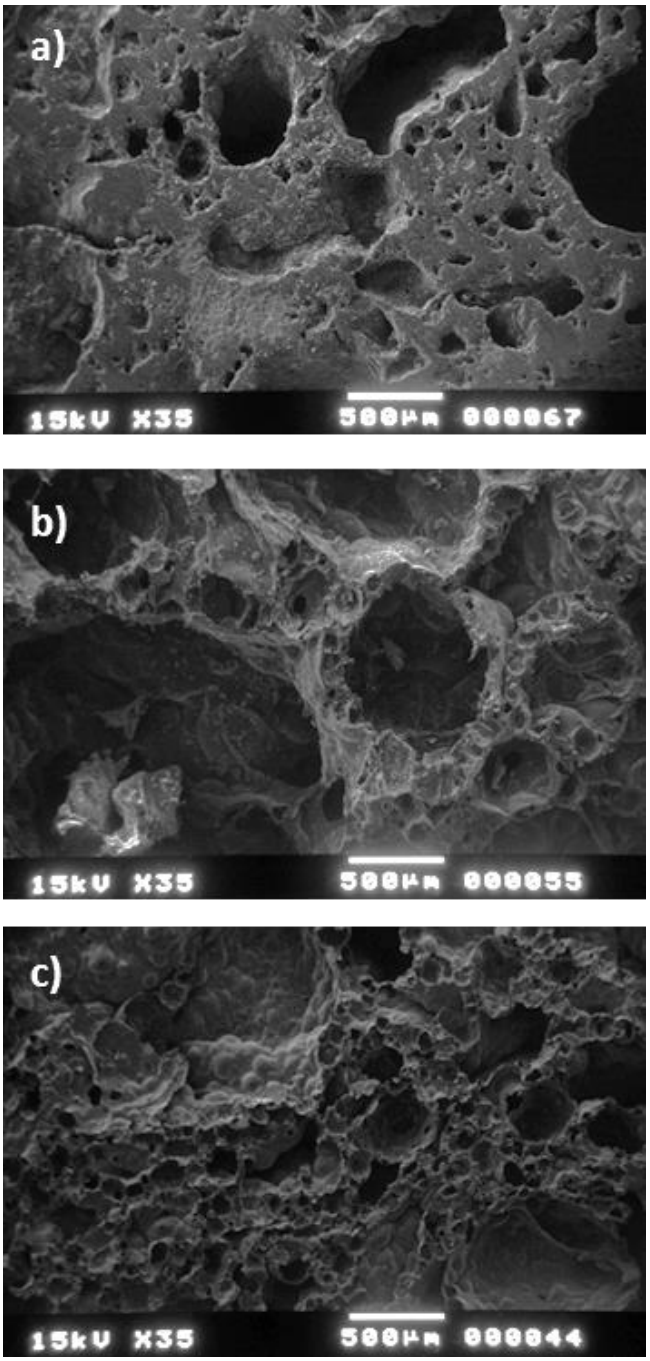

Fig. 4.3. SEM observations of (a) GP-2.5-0.6-10, (b) GP-5-0.6-10, and (c) GP-10-0.6-10 cross-section.

The effect of C_0 on the extent of adsorption of cesium on geopolymer foam at pH of 7 is shown in Figure 4.4. It is evident that the uptake (%) of cesium ions decreases with an increase in C_0. In addition, the adsorbed amount increased with an increase in the adsorbate concentration due to the decrease in the resistance for the uptake of cesium ions from the solution. The adsorption isotherms, q_e versus C_e, of raw material, GP-2.5-0.6-10, GP-5-0.6-10, and GP-10-0.6-10 showed that the adsorption of cesium ion increased with an increase in the amount of silica on geopolymer foams, which provided greater adsorption sites for cesium, due to the increment in the surface area of geopolymer foams. Geopolymer foams with RHA and MK could be compared (Figure 4.5), indicating that the geopolymerization enhanced the capacity of cesium adsorption.

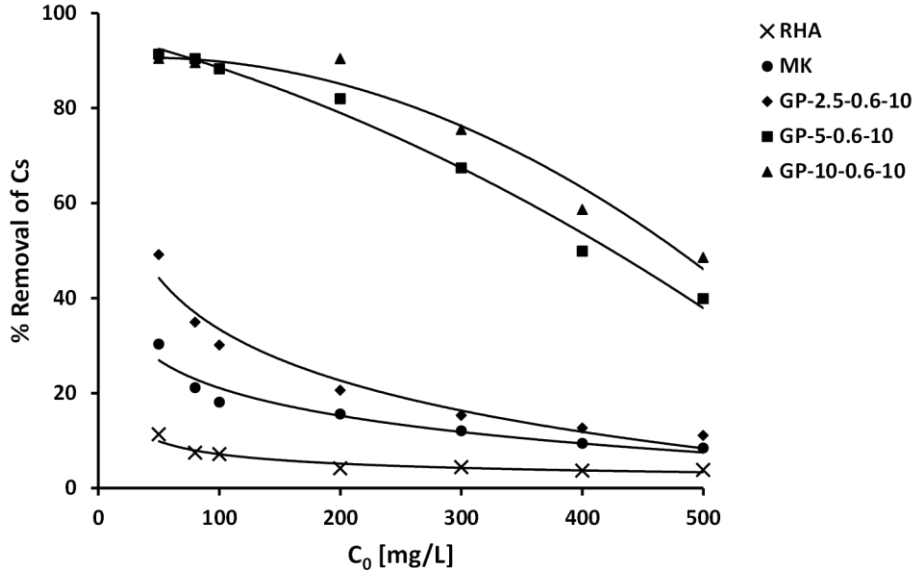

Fig. 4.4. Percentage cesium ion removal onto MK, RHA, and geopolymer foam at pH 7.

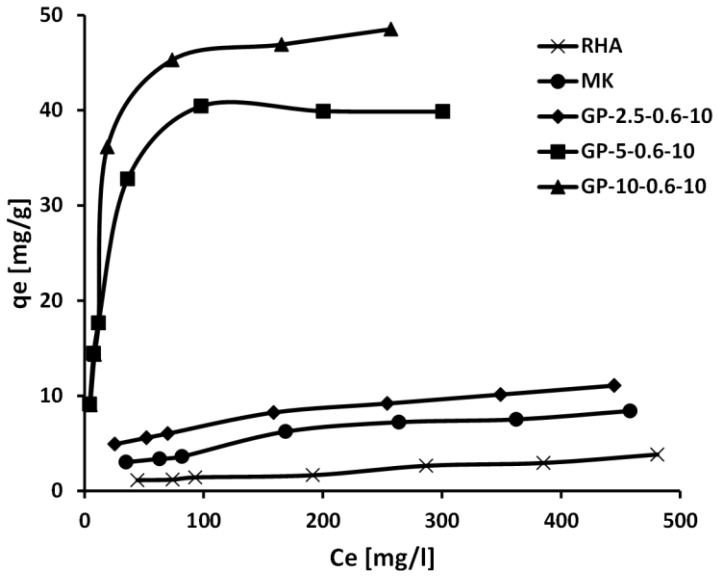

Fig. 4.5. Equilibrium adsorption isotherms of MK, RHA, and geopolymer foam with different amount of RHA at pH 7.

At low adsorbate concentrations, it was noted that the values of q_e rose sharply. At higher values of C_e, the increase in q_e was gradual. Incorporation of the RHA resulted in the enhancement in the adsorptive capacity of the geopolymer foam for the cesium ions.

The experimental results fitted well with the Langmuir equation, showing correlation coefficients of 0.99. The maximum amount of cesium ion adsorption q_m was 11.6 mg/ g for GP-2.5-0.6-10, 41.3 mg/g for GP-5-0.6-10, and 50.8 mg/g for GP-10-0.6-10. The Langmuir constant K_L determined from the intercept and the slope of the plot obtained was 0.022 l/mg for GP-2.5-0.6-10, 0.117 l/mg for GP-5-0.6-10, and 0.082 L/mg for GP-10-0.6-10. The cesium adsorption by geopolymer foams at pH 7 in the presence of 5 and 10 wt% of NaCl was steady, indicating that sodium

concentration had no effect on the cesium adsorption (Table 4.2). This meant that the cesium capture with geopolymer foams might be due to the less effect of electrostatically mechanism.

Table 4.2. NaCl addition to aqueous solution for the adsortion capacity of Cs to geopolymer foams.

Sample	Cs q_{max} [mg/g]		
	0 %wt NaCl	5 %wt NaCl	10 %wt NaCl
GP-2.5-0.6-10	11.6	11.3	12.4
GP-5-0.6-10	41.3	40.0	41.2
GP-10-0.6-10	50.8	48.1	56.0

It is also interesting to compare the adsorption capacity with another material as zeolite. It was noted that the adsorption capacities of the geopolymer foams for the removal of cesium were compared with those of with 34.5 mg/g,[22] RHA with 4.5mg/ g, and MK with 10.4 mg/g at pH 7. Apparently the geopolymer foams GP-5-0.6-10 and GP-10-0.6-10 showed higher capacity of 41.3 and 50.8 mg/g, respectively, for cesium.

4.3 Conclusion.

In conclusion, the synthesis of geopolymer foams from a mixture containing MK and RHA silica under alkaline conditions was successfully achieved. The variation of silica from RH for the synthesis led to important modifications in terms of the formation and structure of the final amorphous products. The removal efficiency

increased with the increment of the silica amount in geopolymer. GP-10-0.6-10 showed high absorption of cesium in water solution. The study indicated the suitability of application of the geopolymer foam for wastewater treatment.

4.4 Reference.

1. Gu BX, Wang LM, Ewing RC. The e ect of amorphization on the Cs ion exchange and retention capacity of zeolite-NaY. 2000;278:64–72.

2. Wang S, Peng Y. Natural zeolites as effective adsorbents in water and wastewater treatment. *Chem. Eng. J.* 2010;156(1):11–24.

3. Xu H, Van Deventer JSJ. Geopolymerisation of multiple minerals. *Miner. Eng.* 2002;15(12):1131–1139.

4. Xu H, Van Deventer JSJ. The geopolymerisation of alumino-silicate minerals. *Int. J. Miner. Process.* 2000;59(3):247–266.

5. Davidovits J, Quentin S. GEOPOLYMERS Inorganic polymerie new materials. 1991;37:1633–1656.

6. Grutzeck MW, Siemer DD. Zeolites Synthesized from Class F Fly Ash and Sodium Aluminate Slurry. 1997;53:2449–2453.

7. Duxson P, Fernández-Jiménez a., Provis JL, Lukey GC, Palomo a., Deventer JSJ. Geopolymer technology: the current state of the art. *J. Mater. Sci.* 2006;42(9):2917–2933.

8. Jaarsveld JGSVAN, Deventer JSJVAN, Lorenzeni L. The potential use of geopolymeric materials to immobilise toxic metals : part i . theory and applications. 1997;10(7):659–669.

9. Borai EH, Harjula R, Malinen L, Paajanen A. Efficient removal of cesium from low-level radioactive liquid waste using natural and impregnated zeolite minerals. *J. Hazard. Mater.* 2009;172(1):416–22.

10. Monzó M, Vicent M, Palomo A, Barba A. Activación alcalina de metacaolín. Efecto de la adición de silicato soluble y de la temperatura de curado. *Cerámica y Vidr.* 2008;47(1):35–43.

11. Chakraverty A, Mishra P, Banerjee HD. Investigation of combustion of raw and acid-leached rice husk for production of pure amorphous white silica. *J. Mater. Sci.* 1988;23:21–24.

12. Goñi S, Frias M, Vegas I, García R, Vigil de la Villa R. Effect of ternary cements containing thermally activated paper sludge and fly ash on the texture of C–S–H gel. *Constr. Build. Mater.* 2012;30:381–388.

13. Weng L, Sagoe-Crentsil K. Dissolution processes, hydrolysis and condensation reactions during geopolymer synthesis: Part I—Low Si/Al ratio systems. *J. Mater. Sci.* 2007;42(9):2997–3006.

14. Sagoe-Crentsil K, Weng L. Dissolution processes, hydrolysis and condensation reactions during geopolymer synthesis: Part II. High Si/Al ratio systems. *J. Mater. Sci.* 2006;42(9):3007–3014.

15. Zhang YJ, Zhao YL, Li HH, Xu DL. Structure characterization of hydration products generated by alkaline activation of granulated blast furnace slag. *J. Mater. Sci.* 2008;43(22):7141–7147.

16. Detphan S, Chindaprasirt P. Preparation of fly ash and rice husk ash geopolymer. *Int. J. Miner. Metall. Mater.* 2009;16(6):720–726.

17. Della VP, Ku I. Rice husk ash as an alternate source for active silica production. 2002;57(December):818–821.

18. Prud'homme E, Michaud P, Joussein E, Clacens J-M, Rossignol S. Role of alkaline cations and water content on geomaterial foams: Monitoring during formation. *J. Non. Cryst. Solids*. 2011;357(4):1270–1278.

19. Prud'homme E, Michaud P, Joussein E, Peyratout C, Smith a., Rossignol S. In situ inorganic foams prepared from various clays at low temperature. *Appl. Clay Sci.* 2011;51(1-2):15–22.

20. Prud'homme E, Michaud P, Joussein E, et al. Silica fume as porogent agent in geo-materials at low temperature. *J. Eur. Ceram. Soc.* 2010;30(7):1641–1648.

21. Delair S, Prud'homme É, Peyratout C, et al. Durability of inorganic foam in solution: The role of alkali elements in the geopolymer network. *Corros. Sci.* 2012;59:213–221.

22. El-Naggar MR, El-Kamash a M, El-Dessouky MI, Ghonaim a K. Two-step method for preparation of NaA-X zeolite blend from fly ash for removal of cesium ions. *J. Hazard. Mater.* 2008;154(1-3):963–72.

Chapter 5

Summary

Recent researches in geopolymer materials have focused on the synthesis of building materials. However, the problem made cleaning of wastewater interest for development of new adsorbent materials. Therefore, the present thesis would give an potential application for geopolymers. In **Chapter 1** showed how the hazardous heavy metal pollution of wastewater was one of the most important environmental problems throughout the world. A wide range of treatment technologies such as chemical precipitation, coagulation and flocculation for heavy metal removal from wastewater were introduced. The adsorption by geopolymers resulted in an attractive solution, because its application is relatively simple and safe. In **Chapter 2**, the research was performed that the alkali activation of the MK and RHA with different ratio of Si/Al = 3 and 10 and different temperature, resulted in an amorphous material called geopolymer. Here, it is observed that the content of RHA incremented the viscoelastic properties of the geopolymers. The elastic modulus quickly exceeded the viscous modulus, indicating that both materials have a reconstruction on Si and Al species during the geopolymerization process.

In **Chapter 3** described the MK-based geopolymers for targeted adsorbents to heavy metal ion separation. The studies indicated that the separation of metal ions can be effectively conducted by geopolymer adsorbents, especially for Pb^{2+} and Cs^{+}. The geopolymerization process resulted from the dissolution of aluminosilicate

monomers followed by polymerization of theses monomers creates new siloxo (Si-O-) bonding sites. The amount of equilibrium adsorption capacity q_e of metal ions onto the geopolymers increases with increasing RHA content of the geopolymers. The adsorption process was optimized at Si/Al = 2 (Figure 5.1). This may be due to the increasing siloxo sites, which increases adsorption efficiency. Here, the six-membered ring containing two AlO_4 tetrahedra, the excess of the two negative charges are compensated by Pb^{2+} cation. This suggested that the increment of the silica on the framework affects the binding sites of the geopolymer. The difference in behavior of GP-1-0.6-10 and GP-2-0.6-10 indicates the unique structure of the geopolymers.

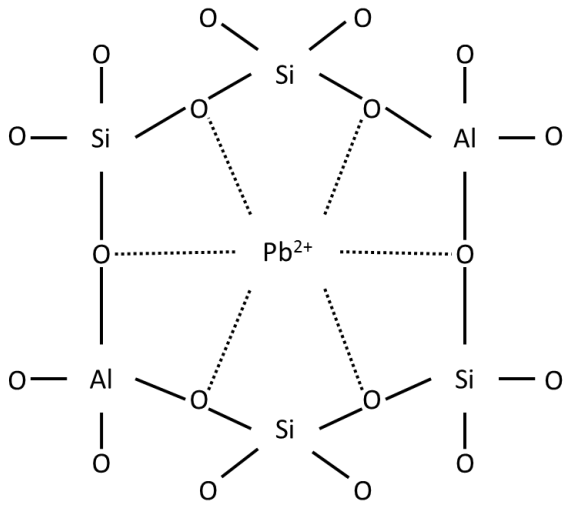

Fig. 5.1. Proposed adsorption mechanism of Pb^{2+} by geopolymers sialate-siloxo.

Meanwhile **Chapter 4** describes the adsorption of cesium by foamed geopolymer based on RHA and MK (Figure 5.2). Here, it was observed that after curing at 150° C a porous material was obtained with excellent properties for cesium adsorption. It was found that the increment of RHA and porosity enhanced the adsorption capacity of the geopolymer

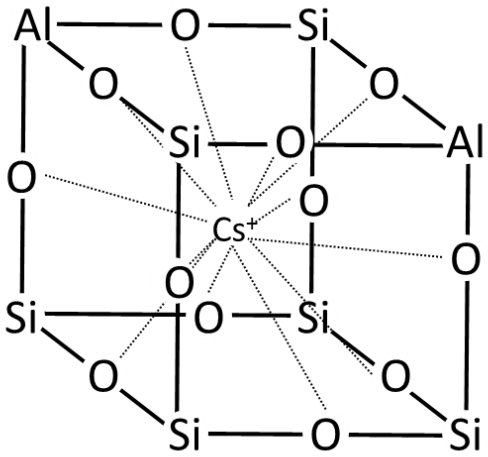

Geopolymer framework

Fig. 5.2. Adsorption of cesium by porous foamed geopolymer based on RHA and MK.

In **Chapter 5** this thesis was summarized.

List of Achievements

Publications paper

López Guzmán Francisco Javier, Sugita Satoshi, Takaomi Kobayashi, "Cesium-adsorbent Geopolymer Foams Based on Silica from Rice Husk and Metakaolin", Chemistry Letters, Vol.43, No.1, 2014, p. 128-130

López Guzmán Francisco Javier, Sugita Satoshi, Tagaya Motohiro, Takaomi Kobayashi, "Geopolymers Using RHA and MK Derivatives; Preparation and Their Characteristics", Journal of Materials Science and Chemical Engineering, Vol. 42, No 5, 2014, p. 35-43.

López Guzmán Francisco Javier, Sugita Satoshi, Tagaya Motohiro, Takaomi Kobayashi, "Metakaolin-based Geopolymers for Targeted Adsorbents to Heavy Metal Ion Separation", Journal of Materials Science and Chemical Engineering. DOI.org/10.4236/msce.2014 [Printing]

Presentation in International Conferences

IV-NATIONAL CONFERENCE ON SCIENCE AND ENGINEERING MATERIALS

Pachuca, Mexico, "Cesim-adsorbent Geopolymer Foams Based don Silica from Rice Husk and Metakaolin", Francisco J. López, Satoshi Sugita, Takaomi Kobayashi, May 2013